Intelligent Monitoring for Fault Detection in Induction Machines

P-1866

A Project Report

Submitted by

S. GOMATHYSELVI - 71205415002

in partial fulfillment for the award of the Degree

of

Master of Engineering

in

Power Electronics and Drives

DEPARTMENT OF ELECTRICAL AND ELECTRONICS ENGINEERING

KUMARAGURU COLLEGE OF TECHNOLOGY

COIMBATORE - 641006

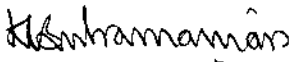## ANNA UNIVERSITY: CHENNAI 600 025

JULY 2007

P-1866

Certified that this project report entitled "**Design and Development of intelligent monitoring for fault detection in Induction Machines**" is the bonafied work of

Mrs. S. Gomathyselvi   -   Register No.   71205415002

Who carried out the project work under my supervision
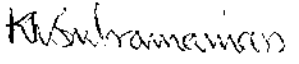
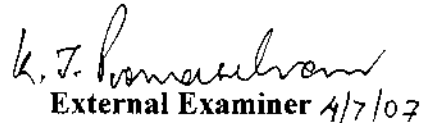Signature of the Head of the Department

Prof. K. Regupathy Subramanian

Signature of the Guide

Mrs. D.Somasundareswari

Certified that the candidate with university Register No. ...71205415002. was examined in Project viva voce Examination held on ..04-07-07......

Internal Examiner

External Examiner 4/7/07

DEPARTMENT OF ELECTRICAL AND ELECTRONICS ENGINEERING

KUMARAGURU COLLEGE OF TECHNOLOGY

COIMBATORE – 641006

Power Electronic Drives"

ISPSPED '07

Department of Electrical and Electronics Engineering

SONA COLLEGE OF TECHNOLOGY

(NBA Accredited & ISO Certified)
SALEM – 636 005

Certificate

This is to certify that Mr/Ms <u>S. GOMATHYSELVI</u> of

<u>KUMARAGURU COLLEGE OF TECHNOLOGY</u> has participated and

presented a technical paper titled <u>DESIGN AND DEVELOPMENT OF</u>

<u>INTELLIGENT MONITORING FOR FAULT DETECTION IN T.M</u>

in the National Conference on **"Innovative Strategies on Power**

Systems and Power Electronic Drives" held on 16th March – 2007.

Coordinator   T.Vijayakumari   Convener   Principal

Induction motors play a very important part in the safe and efficient running of any industrial plant. Early detection of abnormalities in the motor would help to avoid costly breakdowns. Hence, it is essential to check motor condition from time to time. This can be done by various conventional methods but these methods require down time of motors. Among the methods that can be employed for on-line fault detection, neural and fuzzy techniques offer the best solution due to their capacity of handling numerical and heuristic information.

This project aims at the implementation of fuzzy and neural technique for detecting broken rotor bars and broken end-rings in a squirrel cage induction motor. The existence of broken rotor bars and broken end-rings in induction motors can be detected by monitoring any abnormality of the spectrum amplitudes at certain frequencies in the motor current spectrum. These broken rotor bars specific frequencies are settled around the fundamental stator current frequency and are termed lower and upper sideband components.

Hence, this technique uses stator current pattern as inputs. The system will have a single output corresponding to one of the following conditions: no broken bars (healthy condition), number of broken bars, no end ring fault (healthy condition), and number of end-ring sections broken. This approach is validated in a 1HP 415V 50HZ 960-rpm two-pole three-phase induction machine, showing the sensitive frequency components to rotor fault condition. Thus on-line fault detection scheme is done by fuzzy logic approach.

தொழிற்சாலைகளில் மும்முனை இன்டக்சன் மோட்டார்கள் பங்கு மிக முக்கியமானது. ஏனெனில் இந்த வகை மோட்டார்கள் எந்த வகை சுற்றுப்புறச் சூழ்நிலைக்கும் தகுந்தது. இதன் காரணங்களால் இவைகள் அடிக்கடி பழுதடைந்துவிடுகின்றன. தீவிர பழுது அடைந்து பெரும்பான்மையான சேத இழப்பு ஏற்படுவதற்கு முன்னர், ஆரம்ப நிலையிலே பழுதுகளைக் கண்டுபிடிப்பது மிக முக்கியமானது. இதற்கு தொடர்ச்சியாக மோட்டாரின் நிலையினை கண்காணிக்க வேண்டும். ரோட்டரில் ஏற்படும் மிக முக்கியமான பழுதுகளாகிய சட்டங்கள் மற்றும் இறுதிவளையங்கள் உடைதலை கண்டுபிடிப்பதே என் ஆய்வின் நோக்கம். இதற்கு ∴.பஸ்ஸி மற்றும் செயற்கை நியூரஸ் வலைப்பின்னல் முறையினைப் பயன்படுத்தியுள்ளேன்.

உடைந்த சட்டங்கள் மற்றும் இறுதி வளையங்கள், இன்டக்சன் மோட்டாரை சமச்சீர் இல்லா நிலையில் வைக்கின்றன.இதன் விளைவாக தேவையற்ற மின்அதிர்வலைகளை ஸ்டேட்டர் சுற்றுகளில் குறிப்பிட்ட அதிர்வெண்ணில் ஏற்படுத்துகிறது. இதுவே இந்தவகை பழுதுகளை கண்டுபிடிக்கும் காரணிகளாக எடுத்துக் கொள்ளப்படுகிறது. இதன்படி மின்னோட்ட நிறமாலை பகுத்தாய்தல் மூலம் ரோட்டர் பழுதை கண்டுபிடிக்கலாம்.

இத்திட்டத்தில் செயற்கை நியூரல் வலைப்பின்னல் மற்றும் ∴.பஸ்ஸி தத்துவத்திற்கு குறிப்பிட்ட அதிர்வெண்ணில் வரும் மின்னதிர்வலைகளின் மின்னோட்டத்தை உள்ளீடாக செலுத்தம்போது வரும் வெளியீடு மோட்டார் நிலையினை எடுத்துரைக்கிறது. மேலும் ∴.பஸ்ஸி உருப்பு சமன்பாட்டினை மரபியல் விதியைப் பயன்படுத்தி மிகவும் பயன்தக்கதாக உருவாக்கப்படுகின்றது. இதன் மூலம் இயந்திர உதிரிபாகங்களின் பழுதை முன்கூட்டியே அறிந்து மாற்றுவதனால் அதன் செயல்திறன் அதிகரிப்பது மட்டுமின்றி, பழுதுபார்க்கும் செலவும் குறைக்கப்படுகின்றது.

Title	Page no.

CHAPTER 1 INTRODUCTION

i_{rk}	Rotor Circuit Current
i_{rc}	Circulating Current
KVL	Kirchhoff's Voltage Law
f_1	Supply Frequency
f_{sb}	Sideband frequency for broken rotor bar
f_{se}	Sideband frequency for broken end-ring
s	Slip
CT	Current Transformer
CRO	Cathode Ray Oscilloscope
Rms	Root Mean Square
FFT	Fast Fourier Transform
A/D	Analog to Digital Converter
D/A	Digital to Analog Converter
A1, A2	Amplitude at 46Hz, Amplitude at 54Hz
FL	Fuzzy Logic
SCMF	Semi-Circular Membership Function
MF	Membership Function

Induction motors are the workhorses of many different industrial applications due to their ruggedness and versatility. The monitoring, diagnosis and incipient fault detection of motors are important and difficult topics in the engineering field. With proper machine monitoring and incipient fault detection schemes, early warning can be achieved for preventive maintenance, improved safety and reliability of different engineering system operations. The importance of incipient fault detection is found in the cost savings realized by detecting potential machine failures before they occur.

1.1 INDUCTION MOTOR FAULT STATISTICS

Although rotating machines are usually well constructed and robust, the possibility of incipient faults are inherent due to the stresses involved in the conversion of electrical energy to mechanical energy and vice versa. Incipient faults within a machine generally affect the performance of the machine before major failures occur. The use of Induction motors in today's industry is extensive, and the motors can be exposed to different hostile environments, misoperations, and manufacturing defects. Internal motor faults (e.g. Short circuits, ground faults, worn out / broken bearings, broken rotor bars and broken end-rings), as well as external motor faults (e.g. Phase failure, asymmetry of main supply, mechanical overload, and blocked rotors), are inevitable. Furthermore, operation within hostile environments can accelerate aging of the motor and make it more susceptible to incipient faults.

Figure 1.1 shows the fault statistics of induction motor given by Ming XU (1998). The statistical data of failures among utility size motors indicated that 10% of the induction motor failures were rotor related. Rotor related faults in three phase induction motors are due to broken bars and end-rings. The root of the failure is the crack that develops in the rotor bars. The crack may increase its size if left undetected.

Broken bars and end-rings can be a serious problem when Induction motors have to perform hard duty cycles. Broken rotors and end-rings do not initially cause an Induction motor to fail, but they can impair motor performance, lead to motor malfunction, and cause severe mechanical damage to the stator winding if left undetected.

14%   9%

Stator
36%

Bearing
41%
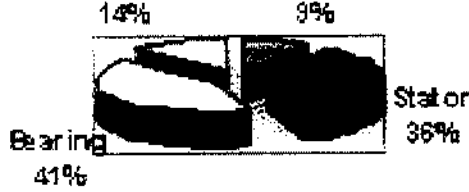
Figure 1.1 Induction Motor fault statistics

1.2 OBJECTIVE

❖ To detect broken rotor bars and end-rings fault in three phase squirrel cage induction motor using neural network and fuzzy logic approach.

❖ Optimization of membership functions in Fuzzy Systems using genetic algorithm.

❖ Using a new membership function of Semi-Circular membership function in Fuzzy system.

❖ On-Line implementation of the fuzzy logic based fault detection scheme.

1.3 LITERATURE SURVEY

Many engineers and researchers have focused their attention on incipient fault detection and preventive maintenance, which aims at preventing major motor faults from occurring.

As pointed out by Peter Vas (1993), the major faults of electrical machines can broadly be classified as the following:

• Stator faults resulting in the operating or shorting of one or more of a stator phase winding,

• Abnormal connection of the stator windings,

• Broken rotor bar or cracked rotor end-rings,

• Static and/or dynamic air gap irregularities,

• Bent shaft can result in a rub between the rotor and stator, causing serious damage to stator core and windings,

• Shorted rotor field winding, and

• Bearing and gearbox failures.

2

- Increased torque pulsations,
- Decreased average torque,
- Increased losses and reduction in efficiency, and
- Excessive heating

Fabricated type rotors have more incidents of rotor bar and end-ring breakage than cast rotors. On the other hand, cast rotors are more difficult to repair once they fail. The reasons for rotor bar and end-ring breakage are several as pointed out by Filippetti et al., 1996. They can be caused by

- Thermal stresses due to thermal overload and unbalance, hot spots or excessive losses, sparking (mainly fabricated rotors),
- Magnetic stresses caused by electromagnetic forces, unbalanced magnetic pull, electromagnetic noise and vibration.
- Residual stresses due to manufacturing problems.
- Dynamic stresses arising from shaft torques, centrifugal forces and cyclic stresses.
- Environmental stresses caused by for example contamination and abrasion of rotor material due to chemicals or moisture,
- Mechanical stresses due to loose laminations, fatigued parts, bearing failure etc.

Different invasive and non-invasive methods for motor incipient fault detection have been reported in (Keyhani et al., 1986).

Invasive techniques require expensive diagnostic equipment and / or off-line fault analysis to determine the motor condition. Many of the invasive techniques available for fault detection and diagnosis in motors, such as radio frequency scheme, particle analysis, vibration analysis and thermal signature (Lyles et al., 1991).

Non-invasive schemes are those, which are based on easily accessible and inexpensible measurements to predict the motor condition without disintegrating the motor structure. These schemes are most suitable for on-line monitoring and fault detection purposes. Many of the inexpensive and non-invasive techniques available for fault detection and diagnosis in motors, such as parameter estimation (Keyhani et al., 1986), Stator current spectrum analysis (Benbouzid 1998).

3

high resolution spectrum analysis to detect the $\pm$ 2sf$_1$ sidebands. Monitor the stator core vibration via an accelerometer and perform high resolution spectrum analysis around the rotor slot passing frequencies to detect the $\pm$ 2sf$_1$ sidebands. Monitor the axial flux signal via a search coil around the rotating shaft and perform high resolution spectrum analysis to detect the $\pm$ 2sf$_1$ sidebands. Monitor speed oscillation via a once-per revolution transducer and perform additional processing to display the predicted number of broken rotor bars. (Thomson 1994).

Even though many motor fault detection schemes have been developed and are being extensively used in the industry, they have achieved a certain degree of success. but are either cost inefficient, unreliable or too difficult to use. With the advancement in technologies and multi-disciplinary collaboration, new opportunities have emerged to improve existing fault detection techniques and to drive the fault detection technology forward. One such key advancement in technology is in the area of artificial neural networks (ANN), which has been applied successfully in fields such as fault detection (Chow et al., 1994).

Although the ANN can provide the correct input-output fault detection relation, it is essentially a "black box" device; i.e., it does not provide heuristic reasoning about the fault detection process. Fuzzy logic could be a solution to this problem. Fuzzy logic can easily and systematically transfer heuristic, linguistic, and qualitative knowledge, (preferred by humans) to numbers and quantitative knowledge, (preferred by computers), and vice-versa. This provides a simple method to heuristically implement fault detection principles and to heuristically interpret and analyze their results. (Chow et al., 1994)

1.4 INTRODUCTION TO NEURAL NETWORK

Artificial neural network is motivated by biological nervous system. An ANN is a network of many neurons richly connected and arranged in more layers. There are interconnections only between units of different layers. Laurence Fausett (2004) explains that the artificial neural networks have been developed as generalization of mathematical models of human cognition or neural biology, based on assumptions that:

- Information processing occurs at many simple elements called neurons.

4

multiplies the signal transmitted.

- Each neuron applies an activation function (usually nonlinear) to its net input (sum of weighted input signals) to determine it output signal.

An Artificial Neural Network is characterized by,

- Its pattern of connections between the neurons (called its architecture)
- Its method of determining the weights on the connections (called its training or learning, algorithm), and
- Its activation function

Artificial neural networks consist of many nodes, i.e. processing units analogous to neurons in the brain. Each node has a node function, associated with it, which along with a set of local parameters determines the output of the node, given an input. Modifying the local parameters may alter the node function. Artificial neural networks thus are an information processing system. In this information processing system, the elements called neuron, process the information. The signals are transmitted by means of connection links. The links possess an associated weight, which is multiplied along with the incoming signal (net input) for any typical neural net. The output signal is obtained by applying activations to the net input.

The neural net can generally be a single layer or a multi-layer net. The structure of the simple artificial neural net is shown in figure 1.2.

Figure 1.2 shows a simple artificial neural net with two input neurons (x1, x2) and one output neuron (y). The interconnected weights are given by w_1 and w_2. In a single layer net there is a single layer of weighted interconnections.
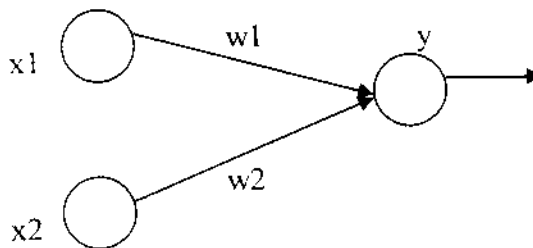
Figure 1.2 A Simple Artificial Neural net

There, the network weight is adjusted based on a comparison of the output and the target, until the network output matches the target.

particular activation function is chosen to satisfy some specification of a problem that the neuron is attempting to solve. There are three most commonly used activation function. They are,

    (a)   Identity activation function

    (b)   Binary step activation function

    (c)   Sigmoid activation function

(a) Identity Function
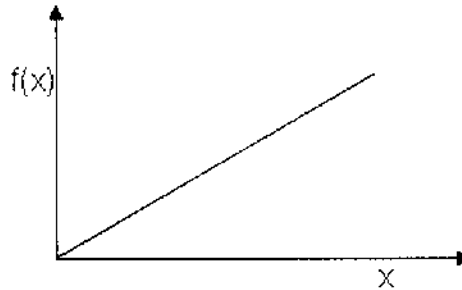
Figure 1.3 Identity Activation Function

Figure 1.3 shows the graphical representation of the Identity activation function. The function is given by,

$$f(x)=x ; \quad \text{for all } x. \tag{1.1}$$

(b) Binary Step Activation Function:

Figure 1.4 shows the graphical representation of the Binary step function. The function is given by,

$$f(x)= \begin{array}{lll} 1: & \text{if} & f(x) \geq \theta \\ 0: & \text{if} & f(x) < \theta \end{array} \tag{1.2}$$
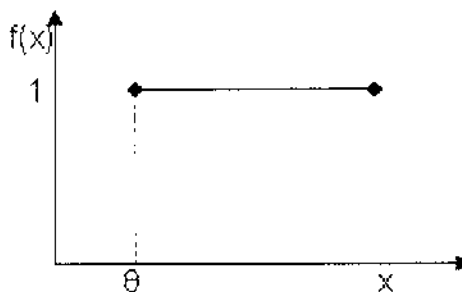
Figure 1.4 Binary Step Activation Function

(c) Sigmoid Activation Function

Figure 1.5 shows the binary sigmoid activation function. This activation function takes the input and squashes the output into the range 0 to 1, according to expression
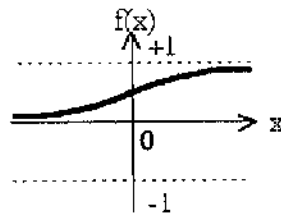
$$f(x) = logsig(x)$$

Figure 1.5 Binary Sigmoid Activation Function

If f(x) is differentiated

$$f'(x) = \sigma\, f(x)[1-f(x)] \qquad (1.4)$$
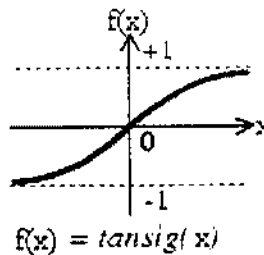
$$f(x) = tansig(x)$$

Figure 1.6 Bipolar Sigmoid Activation Function

Figure 1.6 shows the bipolar sigmoid activation function. The desired range here is between +1 and -1. This function is related to the hyperbolic tangent function. The bipolar sigmoidal function is given as,

$$b(x) = 2f(x) -1 \qquad (1.5)$$

$$b(x) = (1-\exp(-\sigma x)) / (1+\exp(-\sigma x)) \qquad (1.6)$$

$$b'(x) = \sigma /2 \,[\, (1+ b(x))(1-b(x))] \qquad (1.7)$$

1.4.2 LEARNING RULES

The weights and biases of the network can be modified by means of 'learning rule'. This procedure may also be referred to as a training algorithm. The purpose of the learning rule is to train the network to perform some task. Neural networks can be trained to solve problem that are difficult for conventional computers or human beings. There are many types of neural network learning rules. They fall into three broad categories: supervised learning, unsupervised learning and reinforcement (or graded) learning.

7

network, the network outputs are compared to the targets. The learning rule is then used to adjust the weights and biases of the network in order to move the network outputs closer to the targets. An example for the supervised learning is the perceptron-learning rule.

b) Reinforcement learning: This is similar to supervised learning, except that, instead of being provided with the correct output for each network input, the algorithm is only given a grade. The grade is a measure of the network performance over some sequence of inputs. This type of learning is currently much less common than supervised learning.

c) Unsupervised learning: In unsupervised learning, the weights and biases are modified in response to network inputs only. There are no target outputs available. The network learns to categorize the input patterns into a finite number of classes. An example for unsupervised learning algorithm is Adaptive Resonance Theory.

1.4.3 BACK-PROPAGATION NEURAL NETWORK

Back propagation is a systematic method for training multi-layer artificial neural networks. It has a mathematical foundation that is strong if not highly practical. It is a multi layer forward network using extend gradient descent based delta learning rule, commonly known as back-propagation (of errors) rule. Back-propagation provides a computationally efficient method for changing the weights in a feed-forward network, with differentiable activation function units, to learn a training set of input output examples. G.E. Hinton, Rumelhart and R.O.Williams first introduced BPN in 1986. Being a gradient descend method it minimizes the total squared error of the output computed by the net. The network is trained by supervised learning method.

The single-layer perceptron like networks are only able to solve linearly separable classification problems. Multilayer perceptron, trained by BP algorithm were developed to overcome these limitations and is currently the most widely used neural network. In addition, multi-layer networks can be used as universal function approximators. A two-layer network, with sigmoid-type activation functions in the hidden layer, can approximate any practical function, with enough neurons in the hidden layer. The Figure 1.7 shows the Architecture of BP Neural Network.

8
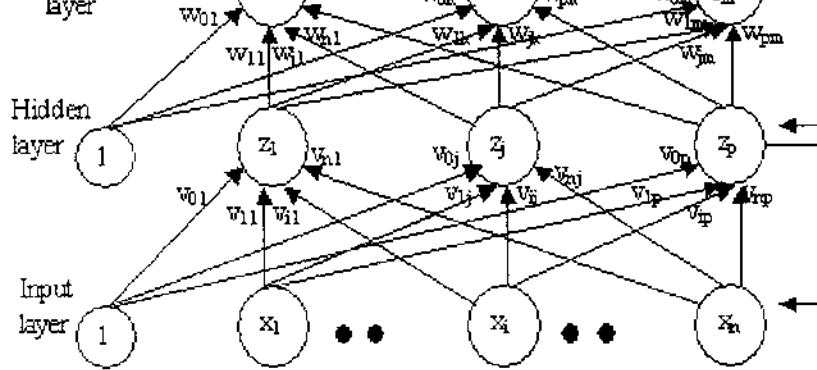
Figure 1.7 Architecture of BP Neural Network

The BP algorithm uses the chain rule in order to compute the derivatives of the squared error with respect to the weights and biases in the hidden layers. It is called BP because the derivatives are computed first at the last layer of the network, and then propagated backward through the network, using the chain rule, to compute the derivatives in the hidden layers.

The BP training algorithm is an interactive gradient algorithm designed to minimize the mean square error between the actual output of a feed-forward net and the desired output. Let x_i, z_j, o_k be the input, hidden and output layer neuron, v_{oj} and w_{ok} are the bias of input and hidden layer, v_{ij} and w_{jk} are the weights of the input to hidden and hidden to output layer.

The BP training algorithm

Step 0: Initialize weights.

Step 1: While stopping condition is false, do steps 2-9,

Step 2: For each training pair, do steps 3-8,

Feed forward:

Step 3: Each input unit (X_i, i=1...n) receives input signal x_i and broadcasts this signal to all units in the layer above (the hidden units).

Step 4: Each hidden unit (Z_j, j =1...p) sums it weighted input signals,

$$Z\_in_j = v_{oj} + \sum_{i=1}^{n} x_i v_{i_j} \,,$$

applies it activation function to compute its output signals,

$Zj=f(z\_in_j)$, and sends this signal to all units in the layer above .

9

$$Y\_in_k = W_{ok} = \sum_{j=1} Z_j W_{jk}$$

And applies its activation function to compute its signals,

$$Y_k = f(y\_ink).$$

Back propagation of error:

Step 6: Each output unit (y_k,k=1...m) receives a target pattern corresponding to input training pattern, computes its error information term ,

$$\delta_k = (t_k - y_k) f'\_(y\_in_k),$$

Calculates its weight correction term (used to update w_{jk} later),

$$\Delta wjk = \alpha \delta kzj ,$$

Calculates its bias correction term (used to update Wok later)

$$\Delta wok = \alpha \delta k$$

Step7: Each hidden unit (Z_j, j =1...p) sums its delta inputs

$$\delta\_inj = \sum_{k=1}^{m} \delta_k w_{jk},$$

multiplies by the derivative of its activation function to calculate its error information term

$$\delta j = \delta\_injf'(z\_inj),$$

Calculates its weight correction term (used to update V_{ij} later),

$$\Delta vij = \alpha \delta jxi,$$

And calculates its bias correction term (used to update V_{0j} later),

$$\Delta voj = \alpha \delta j.$$

Update weights and biases:

Step8: Each output unit (Y_k, k=1...m) updates its bias and weights (j=0...p):

$$W_{jk}(new) = w_{jk}(old) = \Delta wjk,$$

Each hidden unit (Z_j, j...p) updates its bias and weights (i=0...n);

$$Vij(new) = vij(old) + \Delta vij$$

Step 9: Test stopping condition.

1.4.4 CHOICE OF PARAMETERS FOR NETWORK TRAINING

When the basic BP algorithm is applied to a practical problem the training may take days or weeks of computer time. This has encouraged considerable research on methods to accelerate the convergence of the algorithm. The research on faster

performance of the standard BP algorithm. These heuristic techniques include such ideas varying the learning rate, using momentum and rescaling variables. Another category of research has focused on standard numerical optimization techniques.

1.4.4.1 Learning Rate

The speed of training the BP network is improved by changing the learning rate during training. Increasing the learning rate on flat surfaces and then decreasing the learning rate when slope increases can increase the process of convergence. If the learning rate is too large, it leads to unstable learning. And if it is too small, it leads to incredibly long training times. Hence care has to taken while deciding learning rate. There are many different approaches for varying the learning rate. The learning rate is varied according to the performance of the algorithm. The rules of the variable learning rate BP algorithm are:

1. If the squared error increases by more than some set percentage ξ (typically one to five percent) after weight update, then the weight update is discarded, the learning rate is multiplied by some factor $o < p < l$, and the momentum coefficient γ (if it is used) is set to zero.

2. If the squared error decreases after a weight update, then the weight update is accepted and the learning rate is multiplied by some factor $\eta > 1$. If γ has been previously set to zero, it is reset to its original value.

3. If the squared error increases by less than ξ then the weight update is accepted but the learning rate is unchanged. If γ has been previously set to zero, it is reset to its original value.

1.4.4.2 Momentum Factor

In BP with momentum, the weight change is in a direction that is a combination of the current gradient and the previous gradient. This is a modification of gradient descent whose advantage arises chiefly when some training data are very different from the majority of the data. By the use of momentum larger training rate can be used, while maintaining the stability of the algorithm. Another feature of

trajectory has. The momentum coefficient is maintained with the range [0, 1].

1.5 INTRODUCTION TO FUZZY LOGIC

Fuzzy Logic is particularly good at handling uncertainty, vagueness and imprecision. This is especially useful where a problem can be described linguistically (using words) or, as with neural networks, where there is data and you are looking for relationships or patterns within that data. i.e. It is an approach to uncertainty that combines real values [0...1] and logic operations. Fuzzy logic is based on the ideas of fuzzy set theory and fuzzy set membership often found in natural (e.g., spoken) language. Fuzzy Logic uses imprecision to provide robust, tractable solutions to problems. Fuzzy logic relies on the concept of a fuzzy set. The notation for fuzzy sets: for the member x, of a discrete set with membership μ, we use the notation μ/x. In other words, x is a member of the set to degree μ.

Discrete sets are defined as:

$$A = \mu_1/x_1 + \mu_2/x_2 + \ldots + \mu_n/x_n$$

Fuzzy logic systems are universal function approximators. In general, the goal of the fuzzy logic system is to yield a set of outputs for given inputs in a non-linear system, without using any mathematical model, but by using linguistic rules. It has many advantages. They are

- Fuzzy logic is conceptually easy to understand. The mathematical concepts behind fuzzy reasoning are very simple. What makes fuzzy better is the "Naturalness" of its approach and not its far-reaching complexity.

- Fuzzy logic is flexible. With any given system, it's easy to massage it or layer more functionality on top of it without starting again from scratch.

- Fuzzy logic is tolerant of imprecise data. Everything is imprecise if you look closely enough, but more than that, most things are imprecise even on careful inspection. Fuzzy reasoning builds this understanding into the process rather than tacking it onto the end.

- Fuzzy logic can model nonlinear functions of arbitrary complexity. You can create a fuzzy system to match any set of input-output data. This process is made particularly easy by adaptive techniques like Adaptive Neuro-Fuzzy Inference Systems (ANFIS), which are available in the Fuzzy Logic Toolbox.

12

impenetrable models, fuzzy logic lets you rely on the experience of people who already understand your system.

- Fuzzy logic can be blended with conventional control techniques. Fuzzy systems don't necessarily replace conventional control methods. In many cases fuzzy systems augment them and simplify their implementation.

- Fuzzy logic is based on natural language. The basis for fuzzy logic is the basis for human communication. This observation underpins many of the other statements about fuzzy logic.

1.5.1 MAMDANI FUZZY LOGIC INFERENCE SYSTEM

Mamdani-type of fuzzy logic controller contains four main parts, two of which perform transformations. The four parts are

- Fuzzifier (transformation 1)
- Knowledge base
- Inference engine (fuzzy reasoning, decision-making logic)
- Defuzzifier (transformation 2)
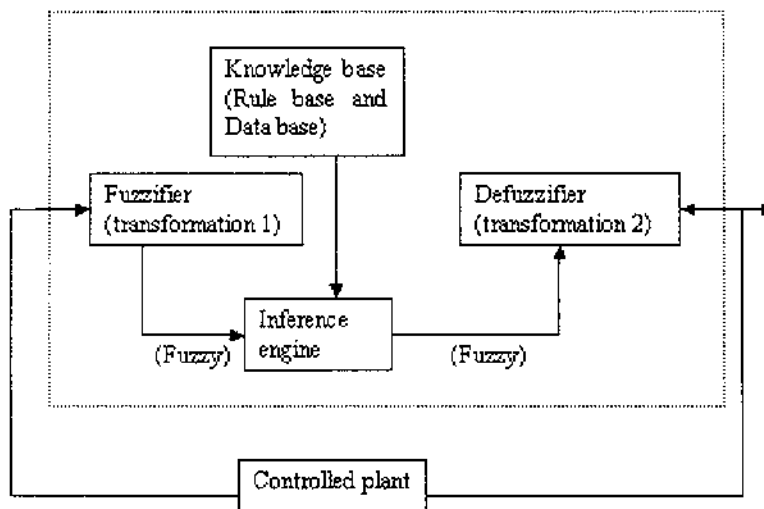
Figure 1.8 Mamdani Fuzzy Logic Inference Systems

1.5.1.1 Fuzzifier

The fuzzifier performs measurement of the input variables (input signals, real variables), scale mapping and fuzzification (transformation 1). Thus all the monitoring input signals are scaled and fuzzification means that the measured signals (crisp input quantities which have numerical values) are transformed into fuzzy

13

belongingness of a quantity to a fuzzy set. If it is absolutely certain that the quantity belongs to the fuzzy set, then its value is 1.

There are many types of different membership functions, piecewise linear or continuous. Some of these are smooth membership functions, e.g. bell-shaped, semicircular, Gaussian etc. and others are non-smooth, e.g. triangular, trapezoidal etc. the choice of the type of membership function used in a specific problem is not unique. Thus it is reasonable to specify parameterized membership functions, which can be fitted to a practical problem.

Semicircular membership function depends on two parameters r, c and can be described as follows by

$$
F(x) = \begin{cases} \left| \sqrt{1 - \dfrac{(c-x)^2}{r^2}} \right| & \textit{if } -r < x < r \\ 0 & \textit{otherwise} \end{cases} \tag{1.8}
$$
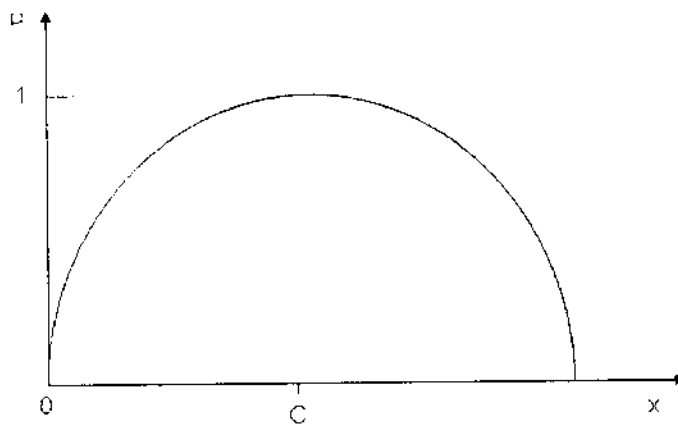
Figure 1.9 Semicircular membership functions

A semicircular membership function is shown in Figure 1.9 is used. The detection of broken rotor bars fault severity is considered by utilizing Mamdani-style fuzzy inference and using as input variables the fault components A_1 and A_2 at frequencies $(1\pm 2s)f$. Very Small, Small, Medium, Large, Very Large are the five membership functions used for the input variable A_1 and A_2. Zero, Incipient fault, One, Two, Three, Four, Five, Six, Seven broken bars are the nine membership functions used for the output variable number of broken bar.

14

base. The database provides the information that is used to define the linguistic control rules and the fuzzy data manipulation in the fuzzy logic controller. The rule base specifies the control goal actions by means of a set of linguistic control rules. In other words, the rule base contains rules such as would be provided by an expert. The fuzzy logic controller looks at the input signals and by using the expert rules determines the appropriate output signals (control actions). The rule base contains a set of if-then rules. The main methods of developing a rule base are:

- Using the experience and knowledge of an expert for the application and the control goals;
- Modeling the control action of the operator;
- Modeling the process;
- Using a self-organized fuzzy controller;
- Using artificial neural networks;

By considering the two dimensional matrix of the input variables, each subspace is associated with a fuzzy output situation.

1.5.1.3 Inference Engine

It is the kernel of a fuzzy logic controller and has the capability both of simulating human decision–making based on fuzzy concepts and of inferring fuzzy control actions by using fuzzy implication and fuzzy logic rules of inference as shown in Figure 1.10. In other words, once all the monitored input variables are transformed into their respective linguistic variables, the inference engine evaluates the set of if-then rules and thus result is obtained which is again a linguistic value for the linguistic variable. This linguistic result has to be then transformed into a crisp output value of the fuzzy logic control.
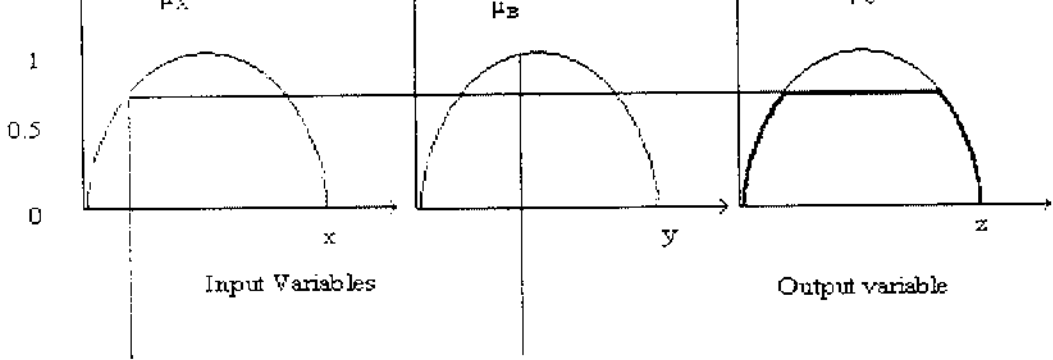
Fig. 1.10 Graphical interpretation of fuzzification, inference

1.5.1.4 Defuzzifier

The second transformation is performed by the defuzzifier, which performs scale mapping as well as defuzzification. The defuzzifier yields a non-fuzzy, crisp control action from the inferred fuzzy control action by using the consequent membership functions of the rules. There are many defuzzification techniques. They are centre of gravity method, height method, mean of maxima method, first of maxima method, sum of maxima.

In this project centroid method defuzzification technique is used as shown in Figure 1.11. Mathematically this center of gravity is expressed as

$$COG = \frac{\int_a^b \mu_A(x)\, x\, dx}{\int_a^b \mu_A(x)\, dx} \tag{1.9}$$
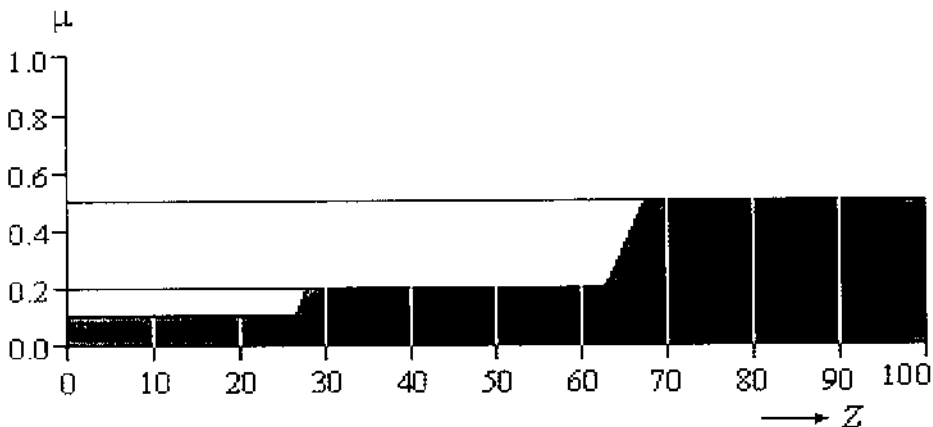
Figure 1.11 Centroid Defuzzification Method

16

Chapter 1, Introduction

Deals with the problems that occur in the induction machines, mainly rotor bar and end-ring failures, the effects produced by them, and techniques used for finding them are discussed. Also provides an overview of the introduction of Neural network and Fuzzy logic.

Chapter 2, Broken Bar/End –Ring Detection In Cage Type Induction Motor

Deals with the various causes of the rotor bar and end-ring failure are discussed. The effects of the broken rotor bar and end-ring are discussed in a single line representation. Detection technique and methodology for finding fault are discussed.

Chapter 3, Experimental Setup for On-line Monitoring

Deals with the sequence of process that is to be carried out to produce the results. The hardware setup for online monitoring for the detection of broken rotor bar and end-ring are discussed. The various components used in the hardware set up are described with their specification and also deals with the software "Real Time Analyzer" used for our project to record the stator current waveforms. The waveforms are analyzed and the harmonic amplitudes under various conditions are tabulated.

Chapter 4, Fault Diagnosis

Explains the simulated result and calculates the percentage of error using both neural network and fuzzy logic approach for rotor fault diagnosis in induction machine. Then compare fuzzy semi-circular membership function with conventional fuzzy membership function. And also compare fuzzy result with neural result.

Chapter 5, Fuzzy Optimization Using Genetic Algorithm

The tuning of membership function in fuzzy logic using genetic algorithm for fault detection is discussed.

Chapter 6, On-line implementation for fault detection

Explains the software used for an On-Line broken rotor bar and end-ring fault detection scheme to three phase squirrel cage induction motor.

Chapter 7, Conclusion

Deals with conclusion and future scope of this project.

Three-phase induction machines are asynchronous speed machines, operating below synchronous speed when motoring and above synchronous speed when generating. It is a well-known fact that induction motors dominate the field of electromechanical energy conversion. The induction machine can operate under asymmetrical stator and/or rotor winding connections during such conditions as: interturn fault resulting in the opening or shorting of one or more circuits of a stator phase winding, abnormal connection of the stator windings, broken rotor bar or end-ring. Asymmetrical operation of induction machines result in unbalanced air gap voltages, consequently unbalanced line currents, increased torque pulsations, and decreased average torque. Consequently, asymmetrical operation of induction machine results in poor efficiency and excessive heating, which eventually leads to the failure of the machine.

2.1 BROKEN ROTOR BAR AND END-RING FAULT MECHANISM

During the start-up period the current in the rotor is at its highest level and this occurs when cooling is minimal and the thermal and mechanical stresses are at a maximum due to the starting currents. Direct on line starting which often occurs on oil production platforms subjects the rotor to a highly stressful condition. The incidence of cracking in the region of the bar to end –ring joint is greater when the start-up time is relatively long and when the start-up time is relatively long and when frequent starts are required as part of a heavy duty cycle. The development of damage to the rotor after cracking of the rotor bar has started can be as follows: the cracked bar overheats around the crack, the bar breaks and arcing occurs; localized heating of the laminations and interbar currents, the adjacent bars carry more current and are subjected to even greater thermal and mechanical stresses during start-up, the rotor laminations can be damaged due to the high thermal stresses, the broken bar can lift out of the slot due to centrifugal forces and can physically damage the stator core and windings.
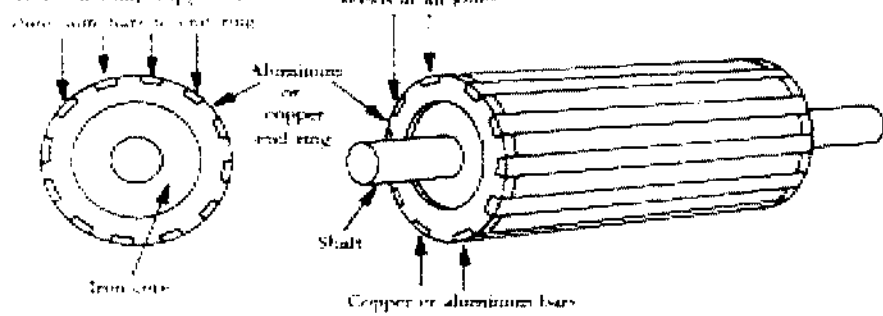
Figure 2.1 Rotor construction of an Induction motor

Almost 90 percent of induction motors are squirrel-cage type, because this type of rotor has the simplest and most rugged construction and is almost indestructible. The rotor as in Figure 2.1, consist of a cylindrical laminated core with parallel slots for carrying the rotor conductors, which are not wire but consists of heavy bars of copper, aluminum or alloys. One bar is placed in each slot rather the bars are inserted from the end when semi-closed slots are used. The rotor bars are brazed or electrically welded or bolted to two heavy and stout short-circuiting end-rings.

The rotor bars are permanently short-circuited on themselves; hence it is not possible to add any external resistance in series with the rotor circuit for starting purposes.

2.3 EFFECT OF ROTOR ASYMMETRY

Under normal operating conditions, an ABC positive sequence of 3-phase balanced terminal (input) voltages impressed upon the three phases, A, B, and C, of the stator armature produces a non-zero forward-rotating field in the airgap of the induction motor. This forward-rotating field in the airgap of the motor consequently induces slip-frequency currents in the rotor bars and connectors, respectively. These induced rotor currents then produce forward-and backward rotating fields in the airgap of the motor. For a symmetrical rotor, the resultant of the backward-rotating fields is zero. while the resultant of the forward-rotating field is non-zero. However, under any abnormal condition that destroys the symmetry of the rotor, a different scenario with regard to the backward-rotating fields arises. In this case, the resultant of the backward-rotating fields is no longer zero. It is the ultimate identification of the effects of this non-zero backward-rotating field that forms the basis for most on-line

19

flows in that bar. The resulting asymmetry in the rotor results in a non-zero backward-rotating field that rotates at slip-frequency speed with respect to the rotor. This non-zero backward-rotating field induces harmonic currents in the stator winding which are superimposed on the stator winding currents at a frequency of $(1-2s)f_1$, where, s is the operating slip and, f_1, is the fundamental stator frequency. These induced currents in the stator windings manifest themselves as a sideband, $(-2sf_1)$, near the fundamental frequency of the power supply.

The flow of current in the rotor circuit can be represented by a single line diagram. This representation is used to describe the modeling of condition Broken Rotor bar and End-ring. The current flow affected by these conditions can be easier to understand with the help of these diagrams.

2.3.1 Modeling of Healthy Induction Motor

The Figure 2.2 shows the current flow representation of a healthy induction motor. In this single line representation there is no broken rotor bars or broken end-rings.
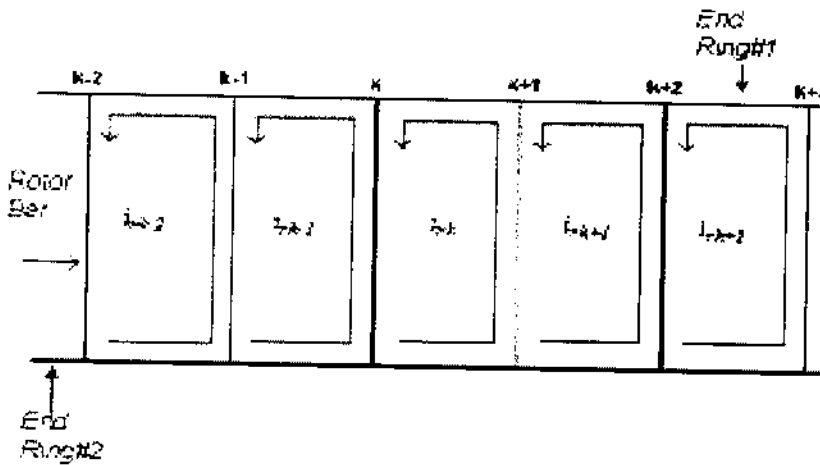
Figure 2.2 Modeling of Healthy Induction motor

The horizontal lines represent the end-rings and the vertical lines represent the rotor bars. Two rotor bars and its connector are represented as a single circuit. And separate currents flow in each circuit and all are equal loops. The rotor current loop is represented as i_{rk} and the representation changes at different bars. The i_{rk} is the Rotor circuit current.

20

and a healthy End-ring (connector). As a result there will be uneven current flow in the rotor-connector circuit where the Broken Rotor Bar is present with respect to other circuits. There are different approaches to the modeling of Broken Rotor Bar.

One approach is to represent the broken bar with a very high resistance leaving the circuit topology unchanged.

And the second approach is to modify the circuit topology by removing the broken bar from the circuit KVL formation. The second approach is better because, (1) the implementation of a broken bar by a very high resistance could introduce numerical ill conditioning and instability, and (2) each time a broken bar is removed, it reduces the simulation time.
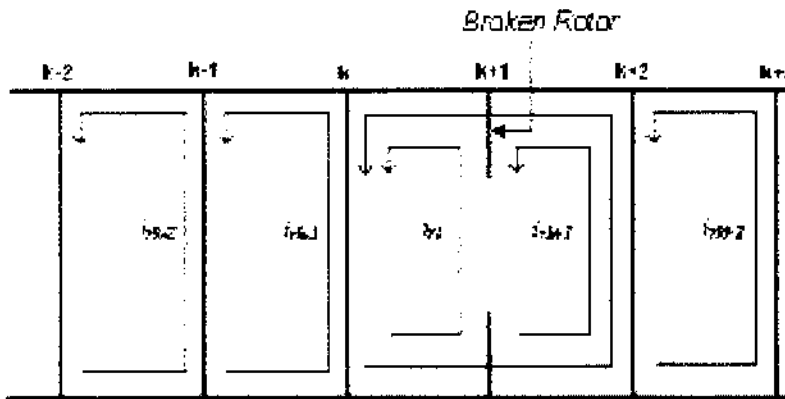
Figure 2.3 Modeling of Broken rotor bar

In the diagram vertical line shows the Rotor bar, where the $(k+1)$th Bar is broken. The figure shows the five adjacent rotor circuits with current labeled, i_{rk-2}, i_{rk-1}, i_{rk}, i_{rk+1}, i_{rk+2}, respectively in which $(k-1)$th bar is broken. Due to the $(k+1)$th broken bar, the rotor circuit currents, i_{rk} and i_{rk+1} , are required to be equal and this current is now forced to flow in the double-width rotor circuit comprising the kth and $(k+1)$th rotor loops as shown in the figure. Broken rotor at different places may lead to more double width rotor current which affects the stator current in turn. So if the number of broken bars is getting increased, these leads to more harmonics in the stator current.

So, proper monitoring must be done to identify the presence of these harmonics. By close examination of the flux plot in an asymmetrical (with broken bars), it can be noticed that the region around the broken bar of the rotor has a high

there is no localized rotor conductor demagnetization effect since these bars carry no slip-frequency currents. This heavy localized magnetic saturation has an irregularity effect on the motor's winding inductance profiles, and an in evitable effect on the stator and rotor core loss distributions. That is, such an event can create a non-uniform distribution of core loss, particularly in the rotor and can result in localized hot spots in the rotor. Such hot spots can lead to excessive heating in the adjacent bars, and thus with time and depending on the duty cycle of the motor, these adjacent bars can become more susceptible to wear, thermal stress and eventual breaking.

2.3.3 Modeling of Broken End-Rings

The modeling approach adopted here is similar to that adopted in the broken bar case. That is, broken rotor end-ring connector segments are not modeled by representing the broken segments by very high resistance. A broken end-ring connector segment is modeled by a non-zero circulating current, i_{rc}, in the connector as shown in the figure.
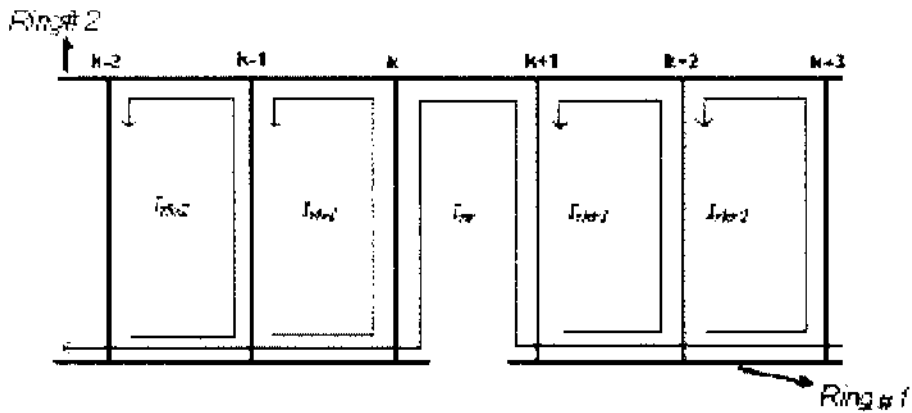
Figure 2.4 Modeling of Broken end -ring

The Figure 2.4 shows the representation of current flow in broken end-ring. The horizontal line shows the two end-rings with a broken section between the rotor bar k and $(k+1)$. It should be noted that no matter where the broken end-ring connector segments are located along the circumference of the rotor, the fault condition is still represented by a single non-zero circulating current, i_{rc}, which flows in all the bars separated by their respective broken connector segments.

These broken connector segments can be got due to high thermal stress or mechanical stress, etc. So broken sections at various connector segments may lead to

connectors.

By observing the magnetic field pattern as in the case of broken bars, it is not symmetrical. The region in the vicinity of the broken connectors has a high degree of magnetic saturation that has distortive effect on winding inductance profiles as like in the broken bar segment.

2.4 FAULT DETECTION SCHEMES

The existence of broken rotor bars and end-rings in induction motors can be detected by monitoring any abnormality of the spectrum amplitudes at certain frequencies in the motor current spectrum. This analysis is called as Motor Current Signature Analysis (MCSA).

2.4.1 Broken Bar Detection Scheme

With a symmetrical cage winding, only a forward rotating field exists. If rotor asymmetry occurs then there will also be a resultant backward rotating field at slip frequency with respect to the forward rotating rotor. As a result, the backward rotating field with respect to the rotor induces an e.m.f. and current in the stator winding at:

$$f_{sb} = f_1(1-2s) \text{ Hz} \qquad (2.1)$$

This eqn.2.1 is referred to as the lower twice slip frequency sideband due to broken rotor bars. There is therefore a cyclic variation of current that causes a torque pulsation at twice slip frequency $(2sf_1)$ and a corresponding speed oscillation, which is also a function of the drive inertia.

This speed oscillation can reduce the magnitude (amps) of the $f_1(1-2s)$ sideband but an upper sideband current component at $f_1(1+2s)$ is induced in the stator winding due to rotor oscillation. The upper sideband is enhanced by the third time harmonic flux. These broken rotor bar specific frequencies are settled around the fundamental stator current frequency and are termed lower and upper sideband components (Kliman et al., 1988, Fillipeti et al., 1996). Those sideband components around the fundamental frequency are given by

$$f_{sb} = f_1(1 \pm 2s) \text{Hz} \qquad (2.2)$$

These two frequency components show predominant variation in their amplitudes and these two components are taken for the analysis under various broken bar conditions.

....   ↑ | | | ↑   ....

(1-4s)f₁   (1-2s)f₁   f₁   (1+2s)f₁ (1+4s)f₁   Frequency (HZ)

Fig. 2.5 Sideband frequencies around the fundamental line frequency

The broken bars also give rise to a sequence of other sidebands given by

$$f_{sb} = (1 \pm 2ks) f_1 \quad ,k=1,2,....,k_n \tag{2.3}$$

And are depicted conceptually in Fig. 2.5.

2.4.2 Broken End-Ring Detection Scheme

As shown in the modeling of the motor, the broken condition in the end-ring will produce backward rotating field, which causes harmonics at specified frequency. Unlike in the case of broken rotor bar condition it will not induce harmonics at both the upper and lower sideband frequencies, but will affect only the lower sideband frequency (Bangura et al., 1999, Demerdash et al., 2000) as given by,

$$f_{se}=(1-2s)f_1 \tag{2.4}$$

The harmonic current amplitude level at lower side band frequency for broken end-ring is higher than that of broken rotor bar because broken cage connectors are far more disruptive on a global scale to patterns of induced current flows in the entire squirrel-cage than broken bars which introduce more localized current flow disruptions.

2.5 METHODOLOGY

The stator current spectrum is converted into an equivalent voltage and recorded by giving it as the input to the microphone input terminal of the PC by means of a stereo cable. The input voltage level to the PC sound card is being adjusted by means of a rheostat to the acceptable level of the sound card. It is normally 1v pk-pk. The current waveforms are recorded for various numbers of broken rotors and end-ring.

Fast Fourier transform is done on the recorded waveforms by means of the FFT analyzer. The output of the FFT analyzer will be in one of the following forms: spectrum, octave band or waterfall model. It will be amplitude Vs frequency graph. The amplitude of the various frequency components is thus displayed in dB. The values can also be recorded by means of using the option data recorder provided by

broken bar and end-ring conditions.

The diagnosis of the faults is done by means of fuzzy logic and neural network approach. Both the methods have been successfully implemented to classify broken rotor bar and end-ring faults by categorizing the $(1+2s)f_1$ and $(1-2s)f_1$ components by a set of rules. Each of these sideband components is described by membership functions like 'very small',' small', 'medium' and 'large', 'very large'. The fuzzy logic system considered is the mamdani type. The fuzzy inference is performed by using the various fuzzy implication methods and the results are being compared in each case. A typical rule might read like" If lower side band is very small and the upper sideband is medium then there is one broken bar." Similarly in neural network using back propagation training algorithm the faults are identified.
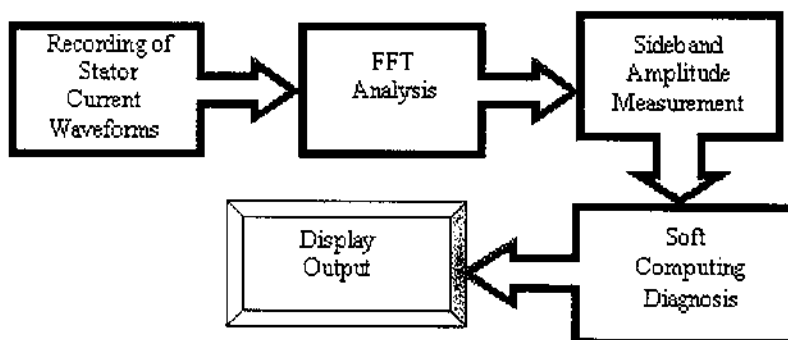
Figure 2.6 Schematic diagram of Methodology

To demonstrate the fault detection scheme, experiments were conducted on the three phase, 1 hp, 415V and 960-rpm induction motor. The motor has 28 rotor bars. To simulate the broken rotor bar fault, a hole is drilled on the rotor bar. With one bar broken, the motor is made to run at rated speed. The stator current is measured. Using the Fast Fourier Transformation (FFT) analyzer, the magnitudes of $(1-2s)f_1$ and $(1+2s)f_1$ are measured. They are denoted as A1 and A2 respectively. The similar procedure is repeated for two to seven broken bars.

3.1 EXPERIMENTAL HARDWARE SETUP
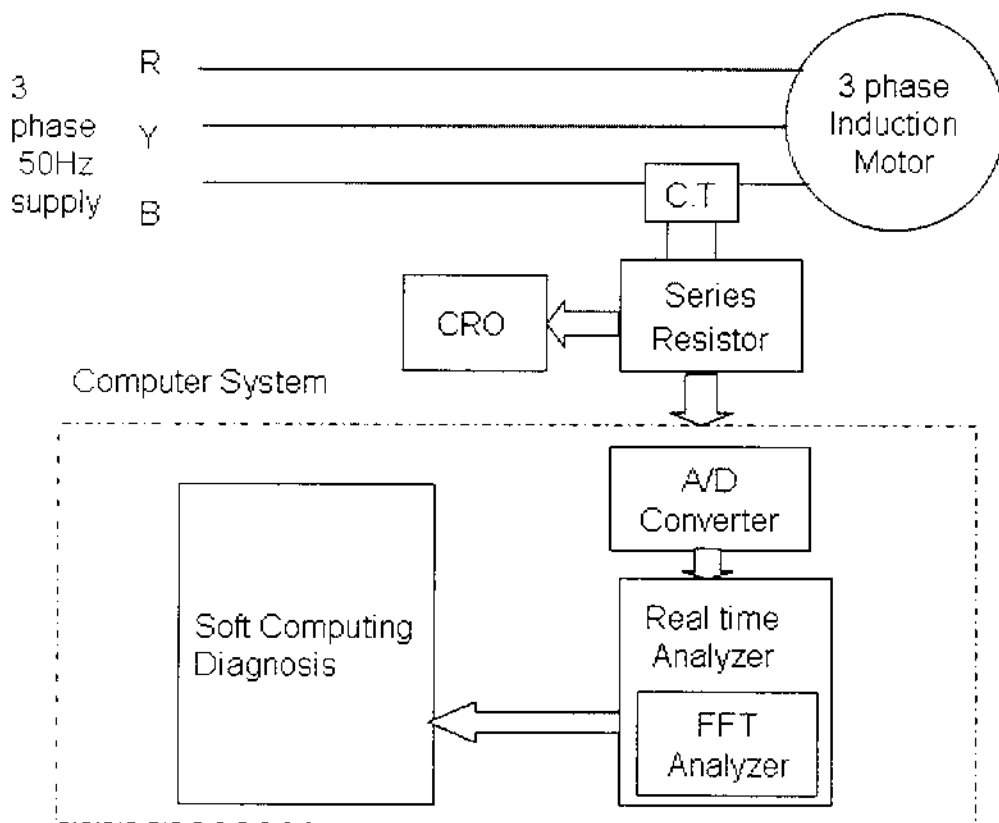
Figure 3.1 Experimental setup for data acquisition
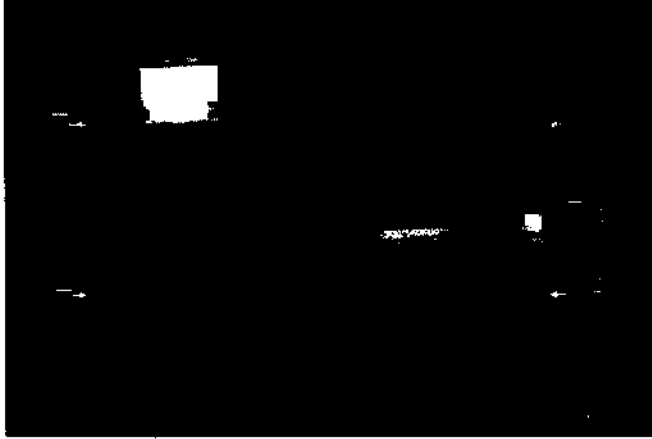
Figure 3.2 Photographic view of the setup

The Figure 3.1 shows the experimental setup used for the project. The 3Ø supply is given to the induction motor. Figure 3.2 from the terminals of the motor, connections are taken from any phase terminal (here phase B) and are connected to a current transformer, which steps down the stator current value. As the computer accepts any signal in the form of voltage, so a rheostat is connected to convert the current to voltage. To set that voltage level to 1v, a CRO is connected across the rheostat to set the range. Across the CRO a stereo cable is connected and is connected to the microphone input of the computer.

The Real Time Analyzer accepts the voltage in the form of sinusoidal waveform and does the FFT analysis and shows the spectrum of the stator current. If any broken sections in the rotor bar or end-ring, it shows the presence of harmonics at the specified frequency in the form of spikes. And to determine the number of broken rotor bars or the number of sections in the end-ring, the fuzzy logic and neural network approach are used.

3.2 HARDWARE COMPONENT SPECIFICATION

3.2.1 Induction Motor

A three phase, 50 Hz squirrel cage induction motor is used. The rotor being casted type made of Aluminum molded bars. Totally there are 28 rotor bars and we have done the analysis for 7 broken bars.

Specification:

Power	:	1HP
Rated voltage	:	415 V

No load current	:	1.7 A
No. of rotor bars	:	28

3.2.2 Current Transformer

Here a current transformer of step down ratio 100:5 is used. The no load line current of 1.7A is being stepped down to 50mA and it is converted in to an equivalent voltage signal by connecting a resistor in serious with the secondary coil.

3.2.3 Rheostat

A rheostat is used to get a voltage output at its terminals. The voltage got will be 1v and it is transferred to the system. The device used here is a 300 Ω rheostat. The voltage is adjusted because the computer accepts any signal only in that range.

3.2.4 Stereo Cable

The input voltage is being given to the PC's microphone input terminal by means of a stereo cable. Since the voltage is already being stepped down to compatible level, there is no need of any ohmic connector to limit the voltage.

3.2.5 A/D Converter

By means of the stereo cable we are giving analog voltage signal to the sound card. There it is converted into a digital form by means of an inbuilt 16 bit A/D converter. Since the precision of the converter is well enough there is no need of any external converter.

3.3 SOFTWARE DESCRIPTION

3.3.1 Real Time Analyzer

The stator current spectrum is converted into an equivalent voltage and recorded in the PC by means of a stereo cable through the microphone input terminal. The input voltage level to the PC sound card is adjusted by means of a potential divider to the acceptable level of the sound card. It is normally 1V (peak to peak). The waveforms are recorded for various numbers of broken bars. In order to perform FFT analysis on the input waveform software "real time analyzer" (figure 3.3) is used. It permits the analog waveform to be directly recorded by the PC. It is a part of "Acoustic Analyzing System" which mainly analyzes sound waveforms. The main advantage of using this software is that it permits the analog waveform to be recorded directly and it is digitized by means of inbuilt A/D converter of the PC's sound card.

Sound Device
Input :Realtek AC97 Audio   ▼   Control Microphone   ▼
Output :Realtek AC97 Audio   ▼   Volume

Input Device
Peak Level Monitor
Input
Output
dB] -80   -70   -60   -50   -40   -30   -20   -10   0

Signal Generator | FFT Analyzer | Oscilloscope | THD Analyzer | Impulse Response | Running ACF | Recorder | Preset | Exit

Fig.3.3 Real time analyzer

The following description specifies about the main parts of the analyzer and its function. The three main functions that are used for this project are Recorder, Oscilloscope, and FFT Analyzer.

3.3.2 Oscilloscope

The Real-time Analyzer is equipped with a Peak Level Monitor. If an oscilloscope is connected to the output terminal of the sound system under tests, problems in transition phenomena related to line connections, earths, and levels will be visible on the oscilloscope screen. Any momentary variances from normal test signals can be investigated immediately.

If the oscilloscope (figure 3.4) is used in combination with the signal generator, it becomes possible to easily check for distortions caused by errors in dynamic ranges for A/D-D/A converters or various types of built-in PC analog amps. From the results of these checks, the user can adjust the software volume on the software mixer, or the program volume on the A/D-D/A converters. Confirmation of the accuracy of these signals is a fundamental rule of measurement.

The real-time analyzer software can measure not only sound but also voltage in small electronic circuits. Actually, the soundcard can input any electric signal, though the attenuator is needed if the signal voltage exceeds the maximum voltage of the soundcard. Here a potential divider is being used to step down the voltage level.
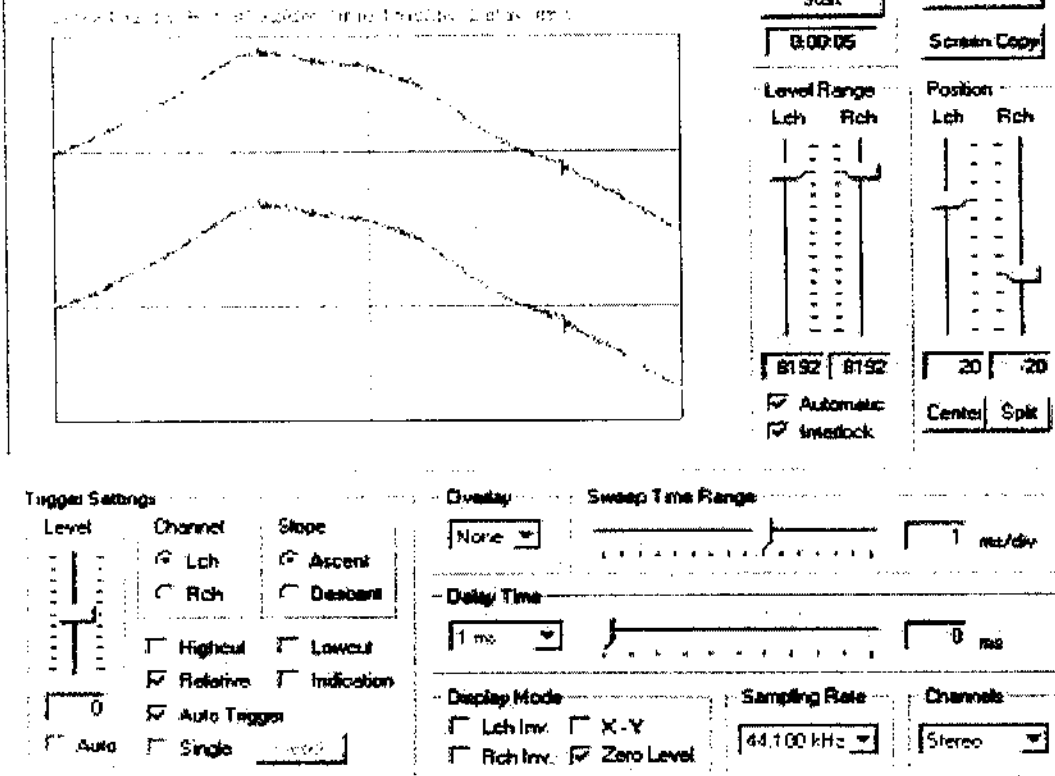
Fig 3.4 Oscilloscope

3.2.3 Recorder

The stereo cable carries the voltage across the rheostat to the computer. The amplitude waveform is recorded and saved in this analyzer. During the online monitoring period the recorder mode is selected to record the waveform and that can be recorded for sufficient time (sec).
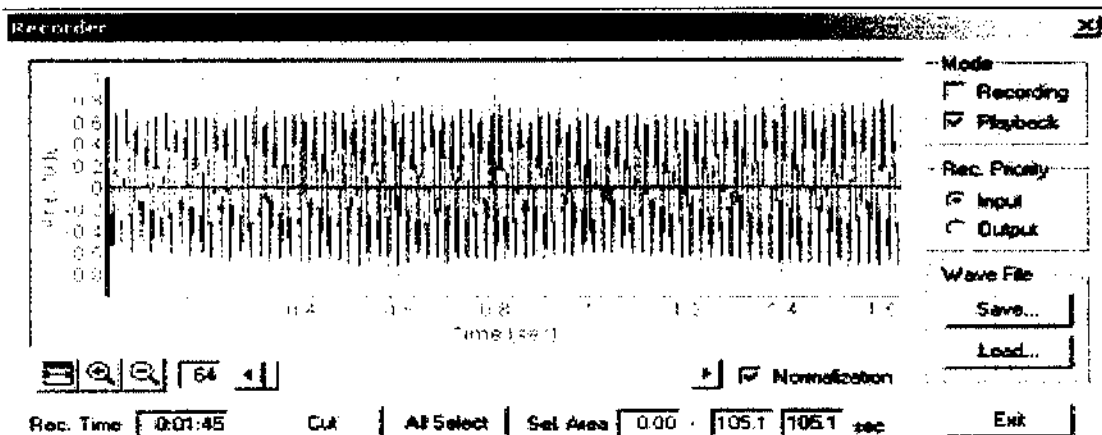
Figure 3.5 Recorder

corresponding waveform is recorded.

3.2.4 FFT Analyzer

By means of FFT analyzer we can perform Fast Fourier Transform on the recorded waveform. The amplitudes of various frequency components are displayed. The displayed data can also be recorded every second. We can see the displayed waveform in the form of octave band, waterfall, correlation, spectrogram, power spectrum and phase. Calibration can also be performed in this FFT analyzer. This can give a clear indication of the amplitude level at each frequency. The mouse pointer can be used to indicate the amplitude level at required frequency i.e. at 46 and 54Hz. When using the octave band, the data record can be used to record the amplitude level at each frequency during the entire time (sec) period of run. A separate screen copy can be got to view the spectrum wave.
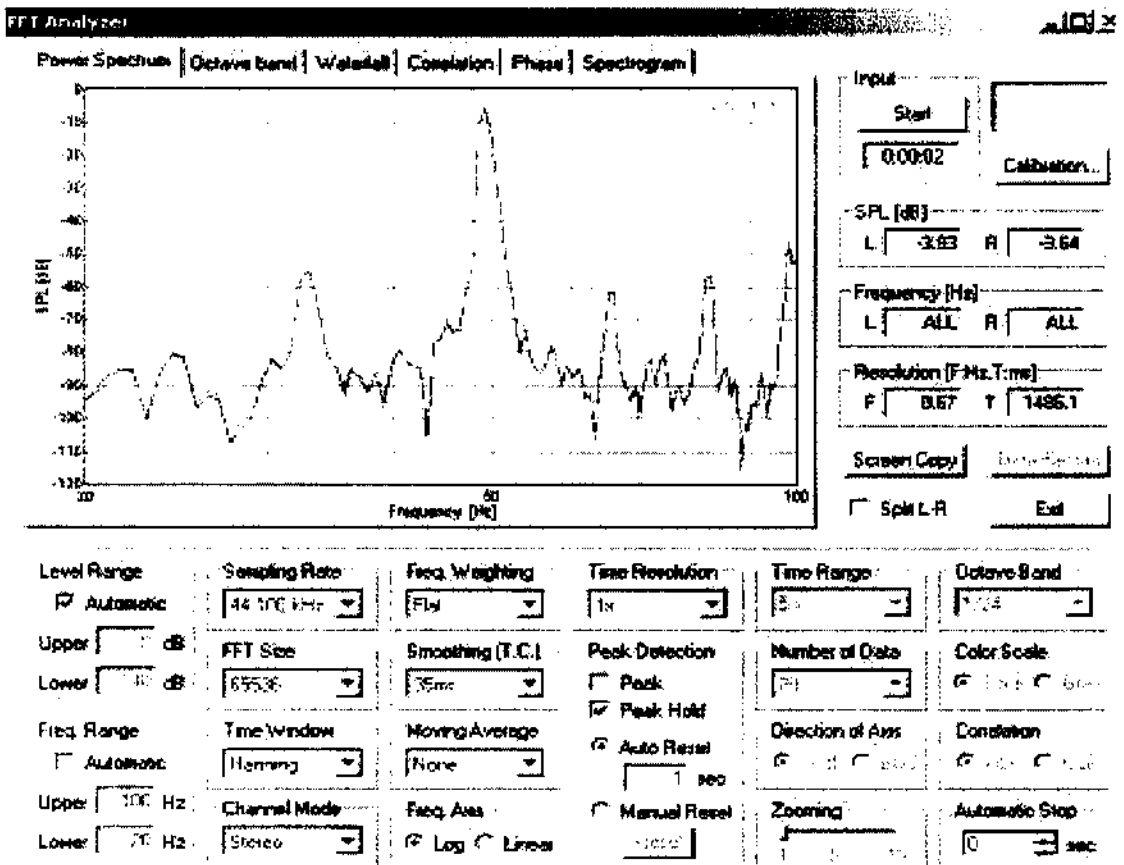
Fig 3.6 FFT Analyzer

3.4.1 Broken Rotor Bar on No-Load condition

The healthy condition of induction is made to run and its corresponding waveform and amplitude level is found out. After that, the rotor is removed and holes are made in the rotor bars and the motor is brought to unsymmetrical condition. The fault condition of the rotor bars can be seen in the figure 3.7. And then the motor is made to run and the corresponding amplitude waveforms and amplitude level is found. The process is continued for many broken rotor bars. Thus the amplitude table is got for various broken bar conditions. The harmonic effect can be seen at the frequencies $\pm 2sf_1$. Here f_1 is 50Hz, s=0.04. So the harmonic effect can be seen at the frequencies of 46Hz and 54Hz.
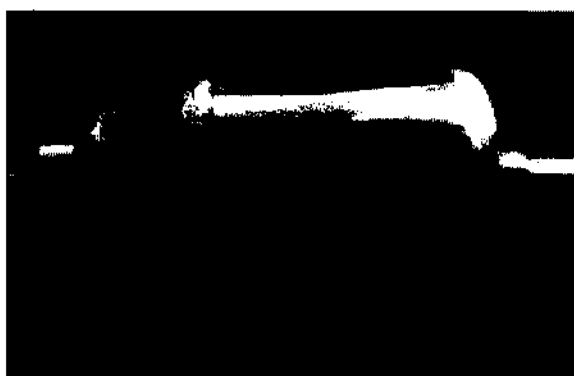
Figure 3.7 Photographic view of broken rotor

Table 3.1 Harmonic amplitudes for no-load condition of broken rotor bars

No. of Broken Rotor Bars	Harmonic Amplitudes at 46 HZ A1 (db)	Harmonic Amplitudes at 54 HZ A2 (db)
0(healthy)	-56.92	-61.8
1	-55.19	-61.58
2	-54.71	-61.06
3	-54.35	-60.32
4	-51.82	-54.81
5	-50.5	-52.4
6	-48	-50
7	-45	-49

present at these frequencies. The figures 3.9 to 3.15 show the indication of harmonics at the frequencies 46Hz and 54Hz. So due to the harmonics, the amplitude level will be higher when compared with the previous value. Therefore, the amplitude level will get higher and higher when there is more number of broken bars.

But it can be seen that there are harmonics present at other frequencies other than 46Hz and 54Hz. Those harmonics may occur due to other failures in the machine.
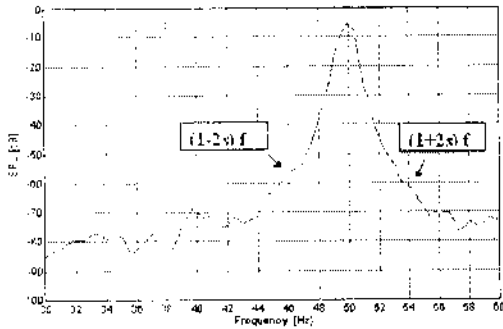
Figure 3.8 Spectrum of a healthy motor

Figure 3.11 Spectrum at three broken bars

Figure 3.9 Spectrum at one broken bar

Figure 3.12 Spectrum at four broken bars

Figure 3.10 Spectrum at two broken bars
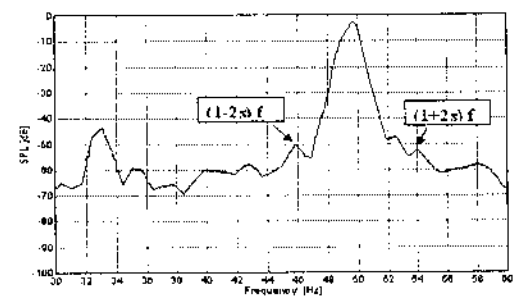
Figure 3.13 Spectrum at five broken bars
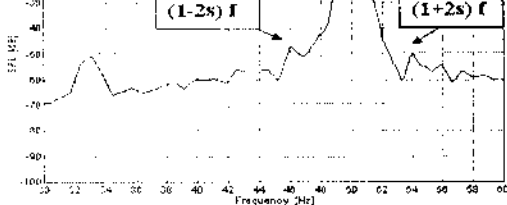
Figure 3.14 Spectrum at six broken bars
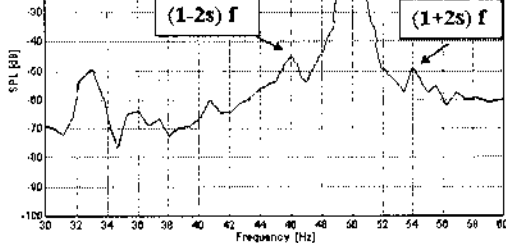
Figure 3.15 Spectrum at seven broken bars

After around seven broken bars, the amplitude variation won't be linear anymore, as it may cause large effects in the machine. So the fault diagnosis is done only for seven broken rotor bar conditions.

3.4.2 Broken Rotor Bar on Load condition

On Load condition the brake drum will be coupled with a spring balance and its amplitude values will be noted.

Table 3.2 Harmonic amplitudes for load condition of broken rotor bar

| No. of Broken Rotor Bars	Harmonic Amplitudes at 46 HZ A1 (db)	Harmonic Amplitudes at 54 HZ A2 (db)
0(healthy)	-56.92	-61.8
1	-53.84	-59.7
2	-53.2	-58.5
3	-52	-57.8
4	-50.3	-53.6
5	-48.5	-51.92
6	-45	-47.5
7	-41.6	-45.7

34
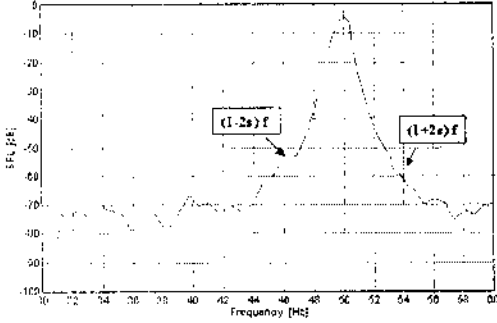
Figure 3.16 Spectrum of a healthy motor
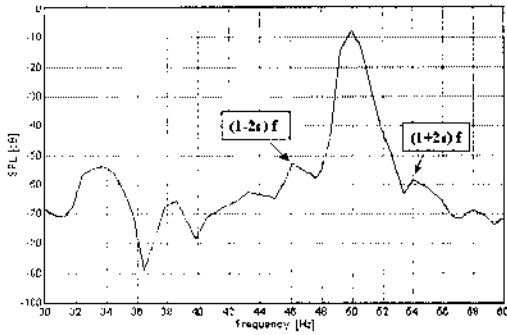
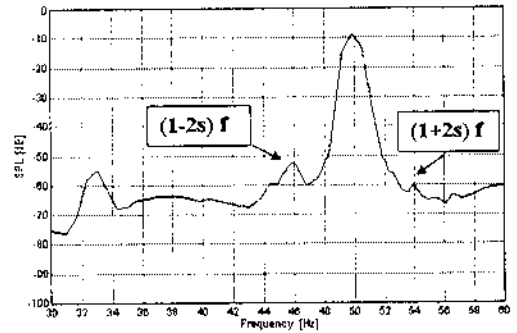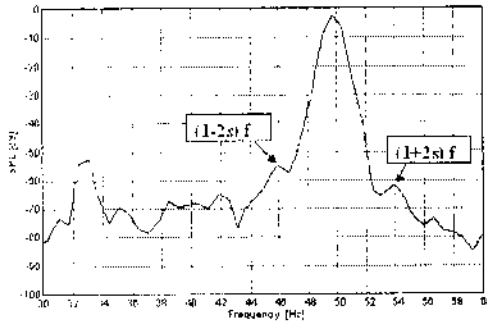Figure 3.17 Spectrum at one broken bar
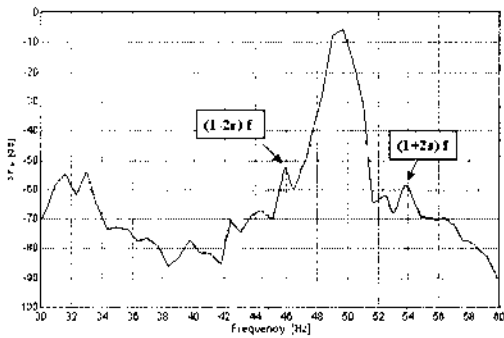
Figure 3.18 Spectrum at two broken bars
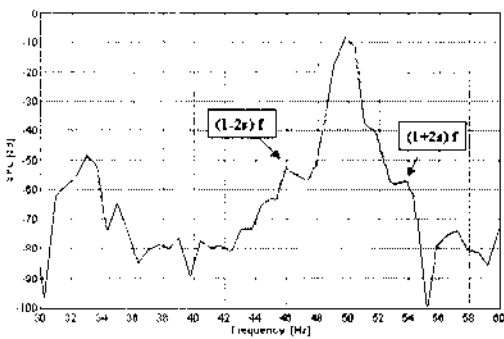
Figure 3.19 Spectrum at three broken bars
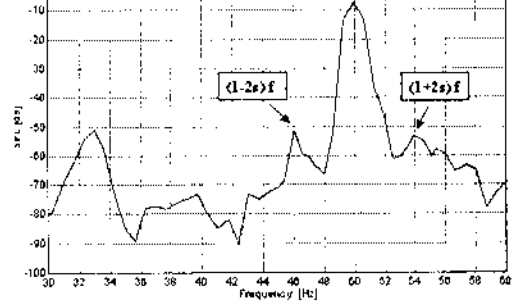
Figure 3.20 Spectrum at four broken bars
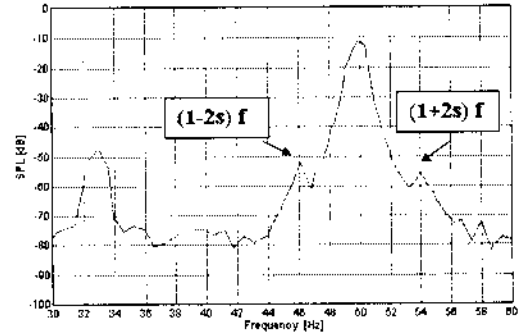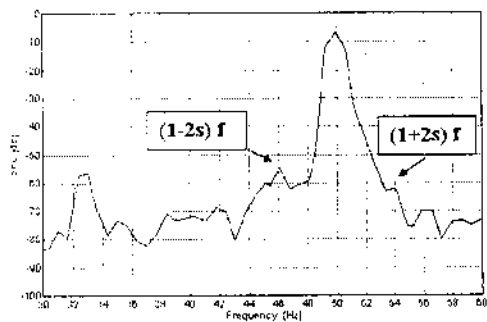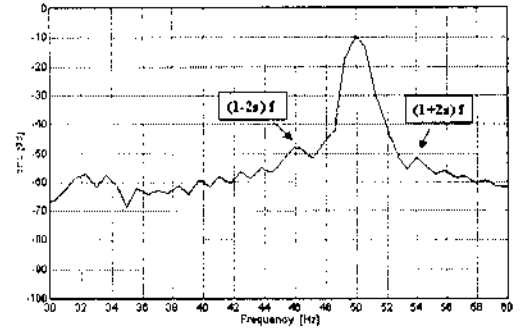
Figure 3.21 Spectrum at five broken bars
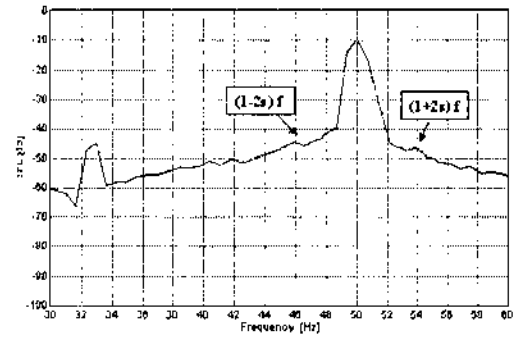
Figure 3.22 Spectrum at six broken bars
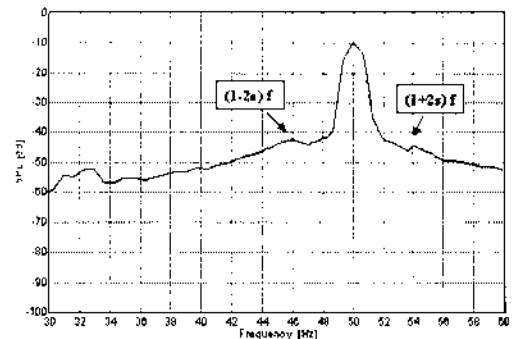
Figure 3.23 Spectrum at seven broken bar

waveform and amplitude level is found out. After that the rotor is removed and the end-ring is then is made to cut using hacksaw blade at a sections. And then the motor is made to run and the corresponding amplitude waveforms and amplitude level is found. The process is continued for many broken end-ring sections. Thus the amplitude table is got for various broken end-ring conditions.
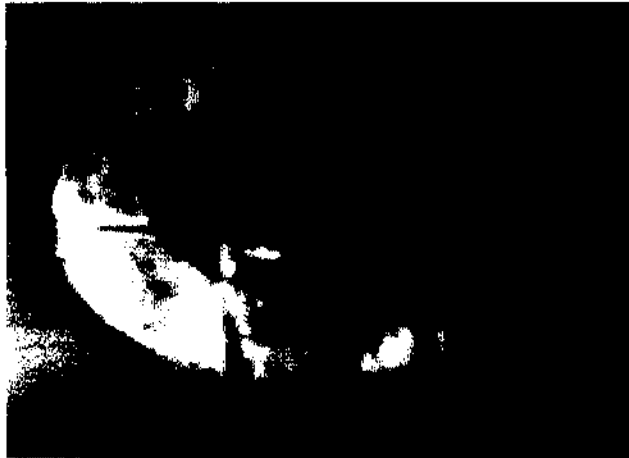
Figure 3.24 Photographic view of broken end-ring

As discussed earlier, any broken (unsymmetrical) condition in the end-ring may cause harmonics at only the frequency **(1-2s) f**, i.e. only the lower side band frequency will get affected. In the above figure of a broken section in end-ring, the spikes are present only at 46Hz frequency.

Table 3.3 Harmonic amplitudes for broken end-ring

No. Of Broken End-ring Sections	Harmonic Amplitudes at 46 HZ A1 (db)
0(healthy)	-56.92
1	-54.56
2	-54.03
3	-49.99
4	-45.6
5	-39.19
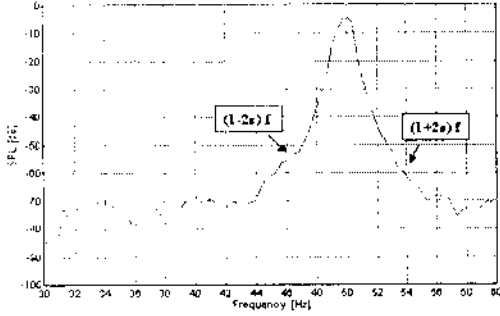
Figure 3.25 Spectrum of healthy condition

Figure 3.26 Spectrum at one broken end-ring section

Figure 3.27 Spectrum at two broken end-ring section

Figure 3.28 Spectrum at three broken end-ring section

Figure 3.29 Spectrum at four broken end-ring section
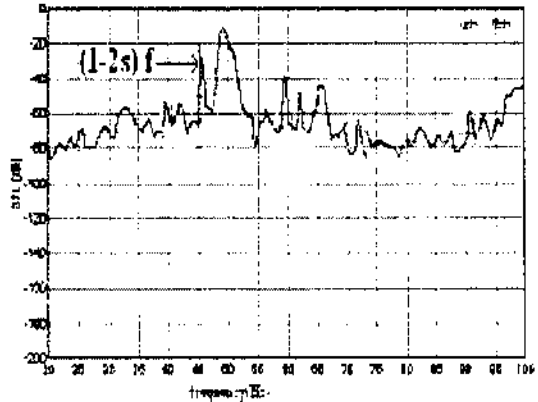
Figure 3.30 Spectrum at five broken end-ring section

The table 3.3 clearly indicates that the harmonic amplitudes level is higher than that due to broken bars. Because broken cage connectors are far more disruptive on a global scale to patterns of induced current flows in the entire squirrel-cage than broken bars, which introduce more localized current flow disruptions. (Bangura et al., 2000).

37

FAULT DIAGNOSIS

Conventional motor fault detection schemes have achieved a certain degree of success, either cost inefficient, unreliable or too difficult to use. With the advancement in artificial intelligence drive the fault detection technology forward.

4.1 NEURAL NETWORK APPROACH

The network consists of two layers namely hidden layer and the output layer. There are eight neurons in the hidden layer. The inputs to the neural network are the amplitudes of A_1 and A_2 and the output is the number of broken bars. The network consists of two input neurons, eight hidden neurons and one output neuron. The BP algorithm is used for training. The log sigmoid activation function is used in the first layer and pure linear activation function is used in the output layer. The learning rate is set to 0.0012, momentum factor is set to 0.8.
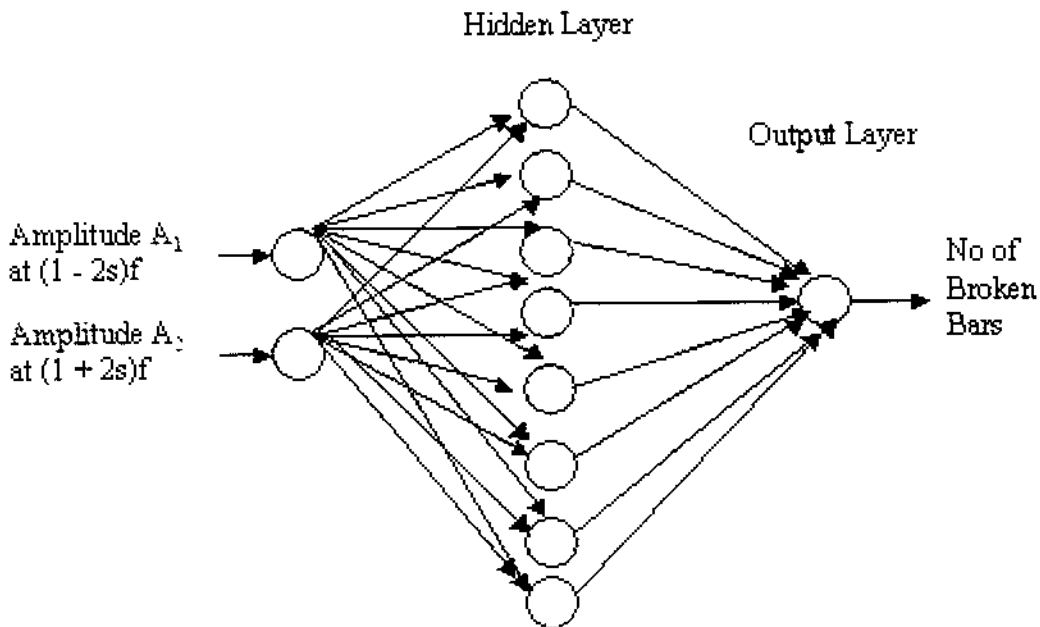
Figure 4.1 Structure of BP Network for fault detection
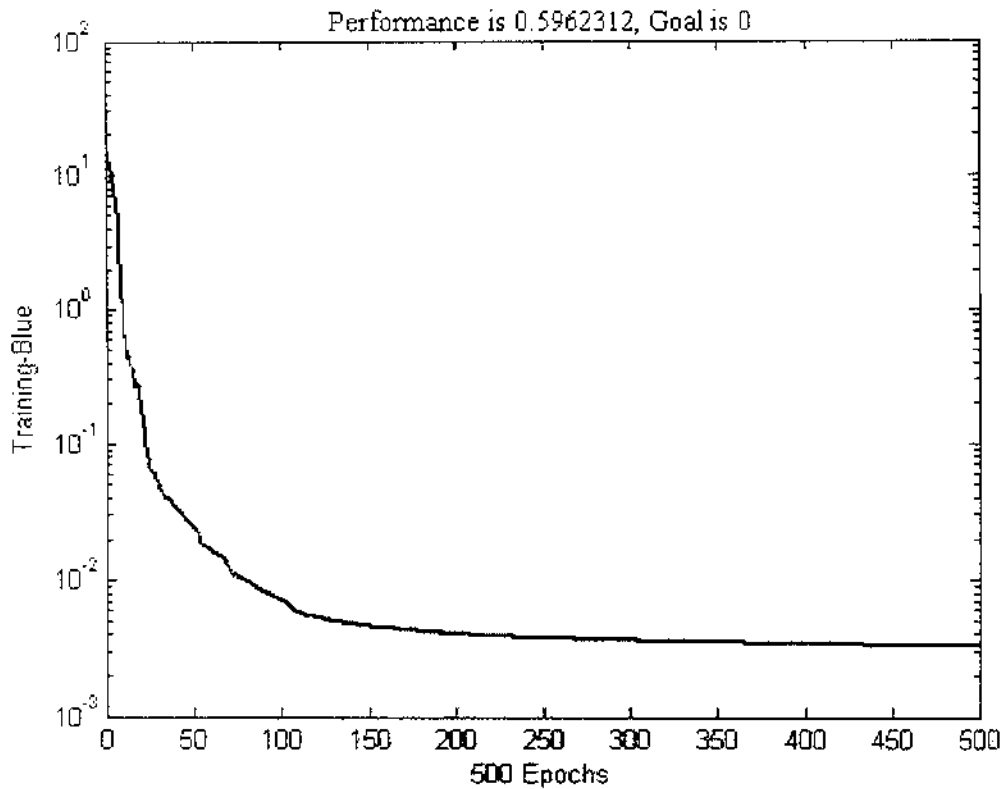
Figure 4.2 Epoch Vs Error Characteristics

Table 4.1 Test results of neural network based fault detection scheme

S.No	A1 in db	A2 in db	Target (No of broken bars)	Actual output	% Error
1	-56.92	-61.8	0	0.0696	0
2	-55.19	-61.58	1	1.0238	2.3
3	-54.71	-61.06	2	2.022	1.1
4	-54.35	-60.32	3	2.9806	0.64
5	-51.82	-54.81	4	4.0047	0.11
6	-50.5	-52.41	5	5.0235	0.47
7	-48	-50	6	6.0024	0.04
8	-45	-49	7	7.0077	0.11
				Average	0.596

Table 4.2 Test results of neural network based fault detection scheme

S.No	A1 in db	A2 in db	Target No of broken bars	Actual output	% Error
1	-55.47	-60.3	0	0.0016	0
2	-53.84	-59.7	1	0.9976	0.24
3	-53.2	-58.5	2	2.002	0.1
4	-52	-57.8	3	2.9991	0.03
5	-50.3	-53.6	4	4.0011	0.0275
6	-48.5	-51.92	5	4.9999	0.002
7	-45	-47.5	6	5.9993	0.011
8	-41.6	-45.7	7	7.0006	0.008
				Average	0.0523
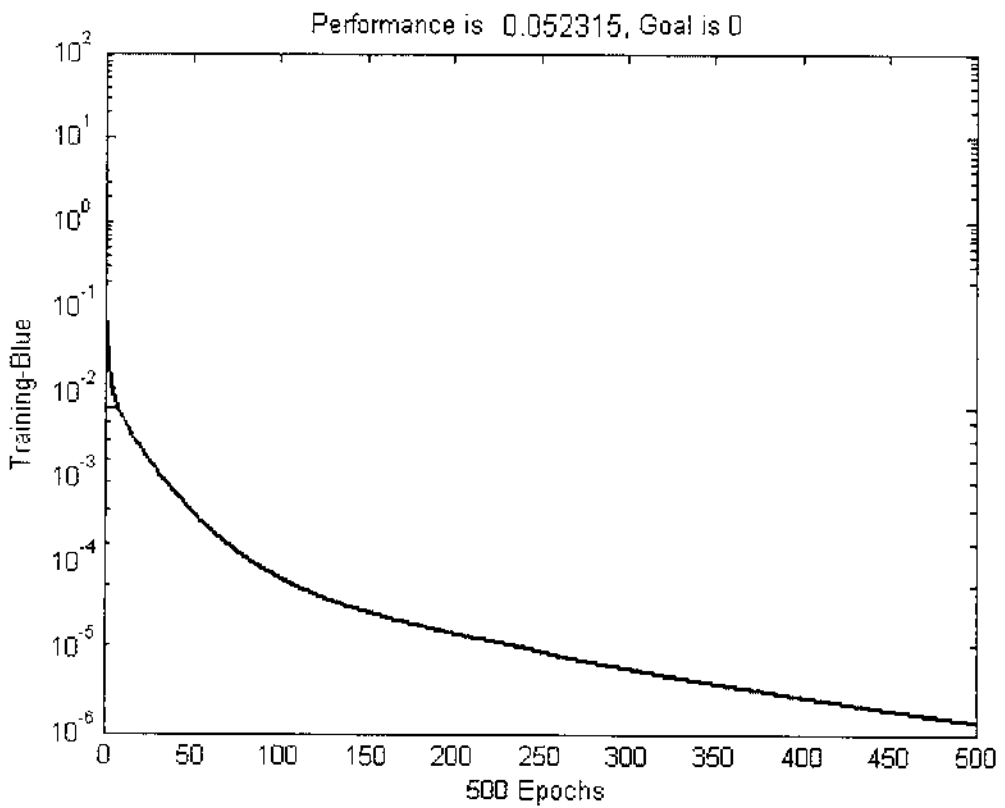
Figure 4.3 Epoch Vs Error Characteristics

conditions. The test results are shown in Table 4.1 and 4.2.

4.1.3 Broken End-ring Sections
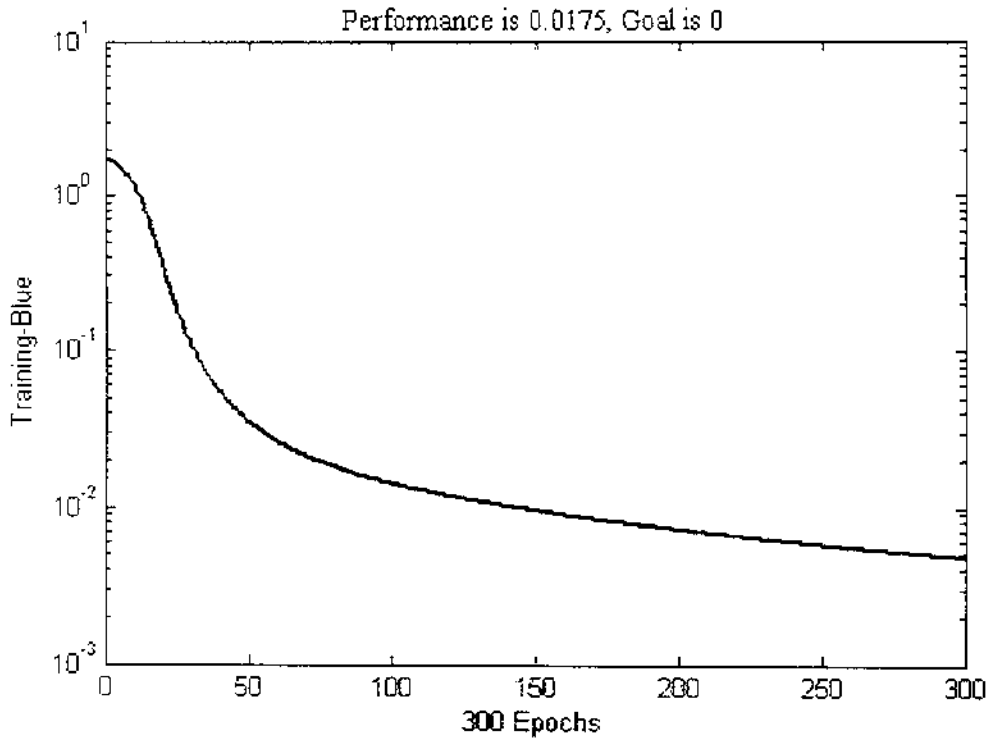
Figure 4.4 Epoch Vs Error Characteristics

Table 4.3 Test results of neural network based fault detection scheme

S.No	A1 in db	Target No of broken connectors	Obtained Value	% Error
0	-56.92	0	0.0347	0
1	-54.56	1	1.001	0.1
2	-54.03	2	1.999	0.005
3	-49.99	3	3	0
4	-45.6	4	4	0
5	-39.19	5	5	0
		Average		0.0175

41
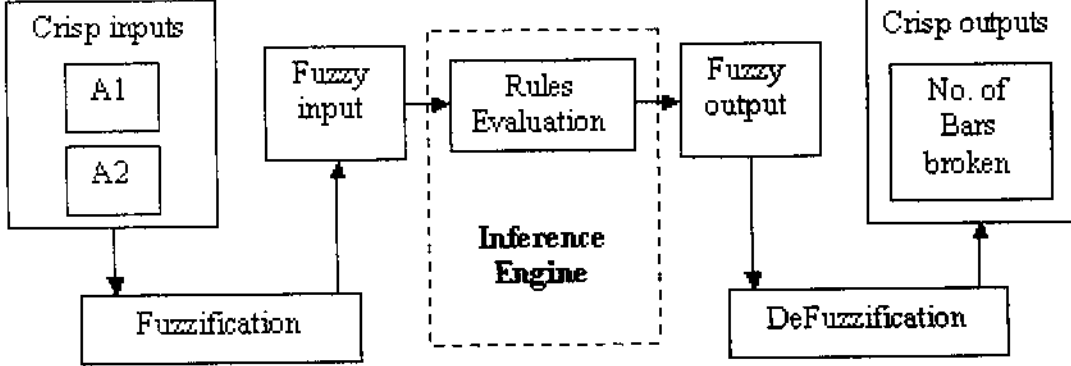
Figure 4.5 Fuzzy System

There are two number of crisp inputs used in this project, A1 and A2, which specifies about the two harmonic amplitudes at the frequency 46Hz and 54Hz. This is in case of broken rotor bar condition. But in the case of broken end-ring condition, there will be only one crisp input. The crisp output in the fuzzy system will display the total number of broken bars and/or the total number of end-ring sections broken.

The inference engine does the fuzzification by using fuzzy concepts. So the crisp inputs have to be converted into fuzzy input. This process is called Fuzzification. Fuzzification converts the numerical data (crisp input) into membership functions (fuzzy input). And also the crisp output displays in the form of numerical data. So the fuzzy output (membership function) from the inference engine is converted into crisp output (numerical data). This process is called Defuzzification. Here Centroid defuzzification technique is used.

The simulation process is done based on the fuzzy implication and fuzzy rules. The rules are framed based on the number of membership functions used in both the input and output. There will be two sets of rules, one for broken rotor bar condition and other for broken end-ring condition. The inference engine simulates based on the rules and displays the output for number of broken rotor bars and number of broken sections in the end-ring.

4.2.1 FAULT DIAGNOSIS FOR BROKEN ROTOR BAR

Two inputs A1 and A2 are used and the rules are framed based on their combination to give the output. In each input functions, five membership functions are implemented.

A1					
VS	0	IF	1	2	3
S	IF	1	2	3	4
M	1	2	3	4	5
L	2	3	4	5	6
VL	3	4	5	6	7

VS: VERY SMALL, S: SMALL, M: MEDIUM, L: LARGE, VL: VERY LARGE, IF: INCIPIENT FAULT

4.2.1.1 Fuzzification with Semicircular Membership Function

As shown in the rules, there will be five membership functions. The width of these five functions will be based on the value of the harmonic amplitudes.
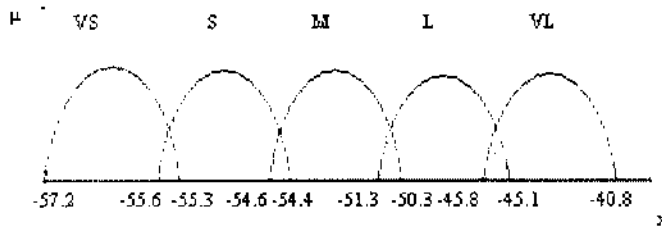
Figure 4.6 Membership Function for A1
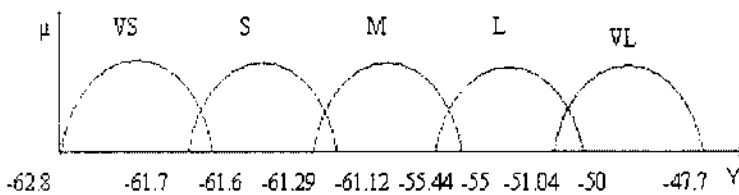
Figure 4.7 Membership Function for A2
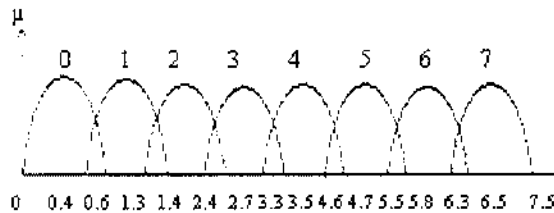
Figure 4.8 Membership Function for output

43

4.2.1.2 Simulation Result

The fuzzy approach is done and the output is got to determine the number of broken rotor bars in no-load condition and load condition. The actual value to be got and the observed value are compared with each other and the percentage of error that arises is calculated. This is done to check the performance and how efficient this approach is.

The error is calculated by the formula,

$$\frac{|\text{Actual value} \sim \text{observed value}|}{\text{Actual value}} * 100$$

The results obtained are shown in the table, in no-load condition…

Table 4.5 Simulation result of broken rotor bar in no-load condition

S.No	A1 in db	A2 in db	Target (No of broken bars)	Actual output	% Error
1	-56.92	-61.8	0	0.0869	0
2	-55.19	-61.58	1	1	0
3	-54.71	-61.06	2	2	0
4	-54.35	-60.32	3	3	0
5	-51.82	-54.81	4	4	0
6	-50.5	-52.41	5	5	0
7	-48	-50	6	6	0
8	-45	-49	7	7.01	0.1
				Average	0.0125

Table 4.6 Simulation result of broken rotor bar in load condition

S.No	A1 in db	A2 in db	Target No of broken bars	Actual output	% Error
1	-55.47	-60.3	0	0.0212	0
2	-53.84	-59.7	1	1	0
3	-53.2	-58.5	2	2	0
4	-52	-57.8	3	3	0
5	-50.3	-53.6	4	4	0
6	-48.5	-51.92	5	5.01	0.2
7	-45	-47.5	6	6	0
8	-41.6	-45.7	7	7	0
				Average	0.025

4.2.1.3 Fuzzification with Triangular Membership Function
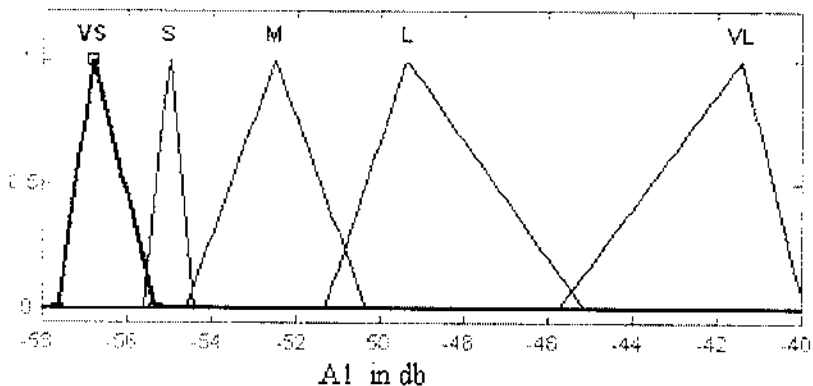
Figure 4.9 Membership Function for A1
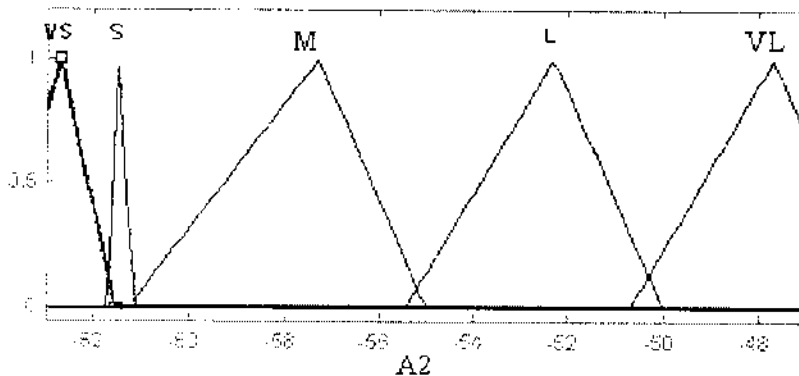
Figure 4.10 Membership Function for A2

45
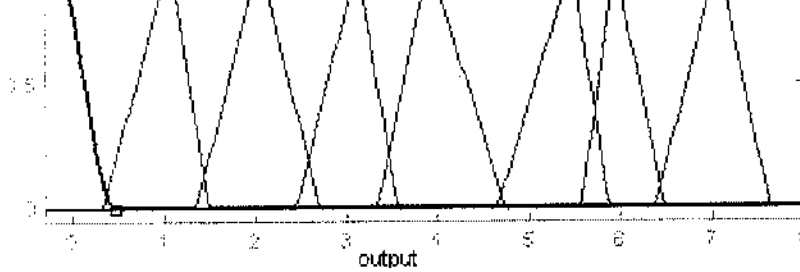
Figure 4.11 Membership Function for output

The results obtained are shown in the table, in no-load condition…

Table 4.7 Simulation result of broken rotor bar in no-load condition

S.No	A1 in db	A2 in db	Target (No of broken bars)	Actual output	% Error
1	-56.92	-61.8	0	0.0269	0
2	-55.19	-61.58	1	1.001	0.1
3	-54.71	-61.06	2	2.02	1
4	-54.35	-60.32	3	3.01	0.3
5	-51.82	-54.81	4	4.02	0.5
6	-50.5	-52.41	5	5	0
7	-48	-50	6	6	0
8	-45	-49	7	7.01	0.1
				Average	0.25

4.2.2 FAULT DIAGNOSIS FOR BROKEN END-RING

The fuzzy logic approach is done to determine the number of section broken at the end-ring. As explained in the effects of broken end-ring, the lower side band frequency will only be disturbed with the harmonics. So the spikes will be present only in the frequency of 46Hz. One input A1 is used as the amplitude and based on the level of that amplitude the number of sections broken at the end-ring is calculated. Six membership functions are used in the input and output to determine the amplitude levels. Fuzzy rules are given as follow

- If input is very very low then healthy machine.
- If input is very low then one end-ring section broken.

- If input is high then four end-ring sections broken.
- If input is very high then five end-ring sections broken.

4.2.2.1 Fuzzification

As shown in the rules there will be six membership functions to determine the number of sections broken in the end-ring. The width of these six membership functions is based on the amplitude levels.
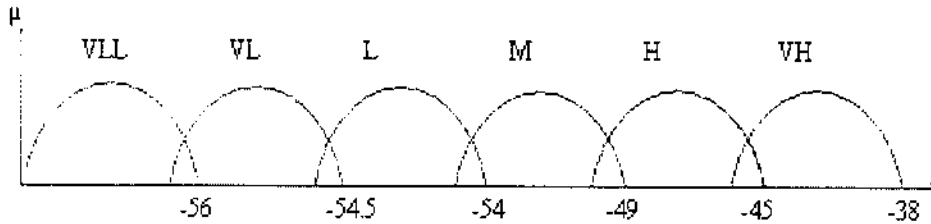
Figure 4.12 Membership function of input A1
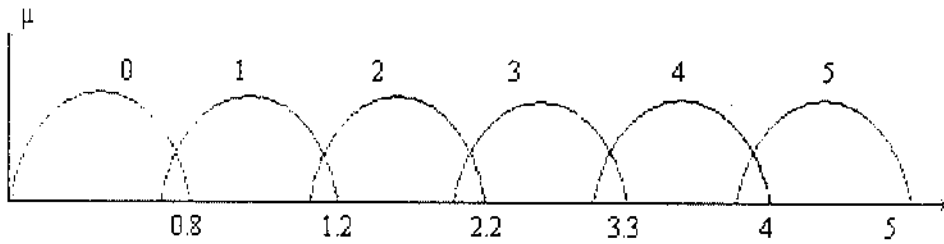
Figure 4.13 Membership function of output

4.2.2.2 Simulation Result

The fuzzy logic approach is done to determine the number of sections broken in the end-ring. The actual value and the observed values are compared and the percentage of error is calculated to find the performance and efficiency of the approach.

	db	No of broken connectors	Value	Error
0	-56.92	0	0.0212	0
1	-54.56	1	1	0
2	-54.03	2	2	0
3	-49.99	3	3	0
4	-45.6	4	4	0
5	-39.19	5	5	0
			Average	0.00

4.3 COMPARISON OF FUZZY LOGIC SCMF WITH CONVENTIONAL MEMBERSHIP FUNCTIONS

The above fuzzy logic procedure is done with various conventional membership functions of triangular, Trapezoidal, gaussian, generalized bell-shaped. For that the same number of inputs and output membership functions are used with same membership function range. The result obtained is tabulated

Table 4.9 Simulation result for broken bar under no-load condition with conventional membership-functions

A1 in db	A2 in db	Target	% Error				
			SCMF	TRIMF	TRAPMF	GBELLMF	GAUSSMF
-56.92	-61.8	0	0	0	0	0	0
-55.19	-61.58	1	0	0.1	0.1	0.6	0.8
-54.71	-61.06	2	0	1	1	1.25	1.3
-54.35	-60.32	3	0	0.3	0.6	1.3	1.4
-51.82	-54.81	4	0	0.5	0.5	1.6	1.7
-50.5	-52.41	5	0	0	0.62	1.8	1.7
-48	-50	6	0	0	0	0.3	0.5
-45	-49	7	0.1	0.1	0.14	0.57	0.5
Average			0.0125	0.25	0.37	0.927	0.9875

4.4 COMPARISON OF NEURAL NETWORK AND FUZZY BASED FAULT DIAGNOSIS SYSTEM

Neural network approach is a black box approach, where the expert knowledge is in the form of weights and biases of the neural network. However, in fuzzy logic based system the actions of a human expert are clearly present in the rule base. From the table, it is inferred that the fuzzy fault diagnosis gives reduced error compared with neural network based diagnosis.

Table 4.10 Comparison of neural network and fuzzy based fault Diagnosis

Condition of Motor	% Error	
	Neural Network Diagnosis	Fuzzy Logic Diagnosis
Broken bars under no-load condition	0.596	0.0125
Broken bars under load condition	0.052315	0.025
Broken end-ring	0.0175	0.0

5.1 INTRODUCTION TO GENETIC ALGORITHM

Genetic algorithms are search algorithms modeled after the mechanics of natural genetics. They are useful approaches to problems requiring effective and efficient searching, and their use is widespread in applications to business, scientific, and engineering fields. In an optimally designed application, Ga's can be used to obtain an approximate solution for single variable or multivariable optimal problems. Before a GA is applied, the optimization problem should be converted to a suitably described function. The corresponding function is called "fitness function". It represents a performance of the problem. The higher the fitness value, the better system's performance. The objective of a GA is to imitate the genetic operation process, e.g., reproduction, crossover, or mutation, to obtain a solution corresponding to the fitness value.

The basic construction of a GA can be simply described as follows.

1) **Define the String of a Chromosome**: The string of searching parameters for the optimization problem should be defined first. These parameters are genes in a chromosome, which can be binary coded or real coded and termed "chromosome". Different chromosomes represent different possible solutions

2) **Define the Fitness Function**: The fitness function is the performance index of a GA to resolve the viability of each chromosome. The design of the fitness function is according to the performance requirements of the problem, e.g., Convergence value, error, rise time, etc.

3) **Generate an Initial Population**: N sets of chromosomes should be randomly generated before using a GA operation. These chromosomes are called the initial population. The size of the population, N, is chosen according to the sophistication of the optimization problem. Generally speaking, the larger values of N require fewer generations to come to a convergent solution. However, the total computation effect depends on N times the generation numbers.

4) **Generate the Next Generation or Stop**: GA's use the operations of reproduction, crossover, and mutation to generate the next generation. From
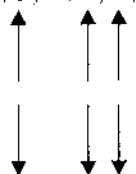
a. **Reproduction**: Reproduction is the operator carrying old strings through into a new population, depending on the fitness value. Stings with high fitness values obtain a larger number of copies in the next generation. An example of such an operation is shown in table 5.1.

b. **Crossover:** Crossover is a recombination operator incorporated with reproduction. It is an effective way of exchanging information and recombining segments from high fitness individuals. The crossover procedure is to randomly select a pair of strings from a mating pool, and then randomly determine the crossover position. An example of the operation is shown in table 5.2.

c. **Mutation:** The mutation operator is used to avoid the possibility of mistaking a local optimum for a global one. It is an occasional random change at some string position based on the mutation probability. An example of the operation is shown in table 5.3.

Table 5.1 Example of the Reproduction of a GA

Old chromosome	Fitness value	New chromosome
[1, 3, 2, 3, 2, 3, 1]	80	[1, 3, 2, 3, 2, 3, 1]
[2, 3, 1, 1, 3, 2, 2]	67	
[3, 1, 1, 3, 2, 3, 3]	56	
[1, 2, 3, 2, 2, 2, 1]	33	

Table 5.2 Example of the Crossover of a GA

Old chromosome	Fitness value	New chromosome
[1, 3, 2, 3, 2, 3, 1]	80	
[2, 3, 1, 1, 3, 2, 2]	67	[2, 1, 1, 3, 2, 2, 2]
[3, 1, 1, 3, 2, 3, 3]	56	[3, 3, 1, 1, 3, 3, 3]
[1, 2, 3, 2, 2, 2, 1]	33	

51

P- 1866

Old chromosome	Fitness value	New chromosome
[1, 3, 2, 3, 2, 3, 1]	80	
[2, 3, 1, 1, 3, 2, 2]	67	
[3, 1, 1, 3, 2, 3, 3]	56	
[1, 2, 3, 2, 2, 2, 1]	33	[1, 2, 1, 2, 3, 2, 1]

5.2 MEMBERSHIP FUNCTION OPTIMIZATION

5.2.1 Tuning Membership Function

In a fuzzy logic system it is possible to obtain final (tuned) membership functions by using genetic algorithms. For this purpose initial membership functions for the various fuzzy variables are assumed and concatenated to make one long string to represent the whole parameter set of the membership functions. A fitness function is then used to evaluate the fitness value of each set of membership functions. Then the reproduction, crossover operators are applied as to obtain the optimal population (membership functions), or more precisely, the final tuned value of the parameter set describing the membership functions used. The Figure 5.1-5.3 show the input variable for the optimization.
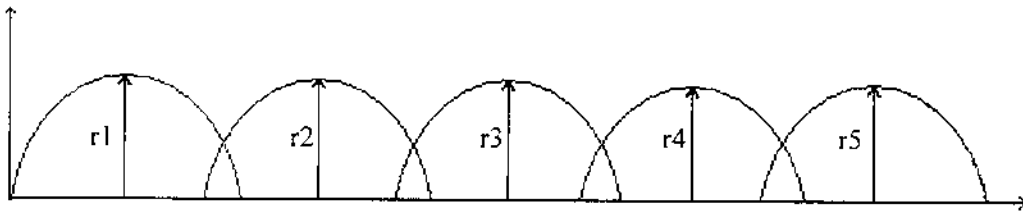
Figure 5.1 Membership Function of Input A_1
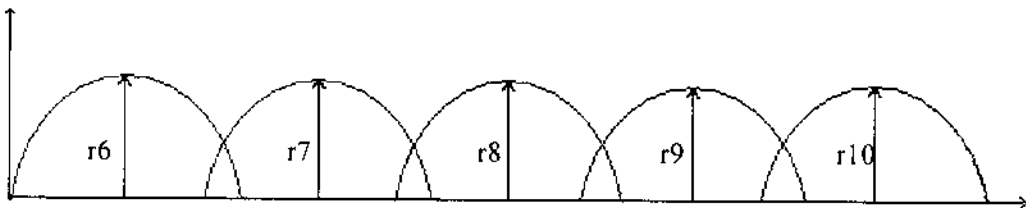
Figure 5.2 Membership Function of Input A_2

$$y = \sqrt{1 - (c-x)^2 \big/ r^2}$$

Step 4   : Using fuzzy rules and defuzzification, find the actual values.

Step 5   : Calculate the fitness function f(x) =target – actual

Step 6   : Termination criteria is f(x) =0. If termination criteria is satisfied, terminate. Else new mating pool is created by Roulette-wheel reproduction method.

Step 8   : Select the swapping pair for crossover and mutation. Then the new population is created.

Step 9   : Repeat the above procedures.
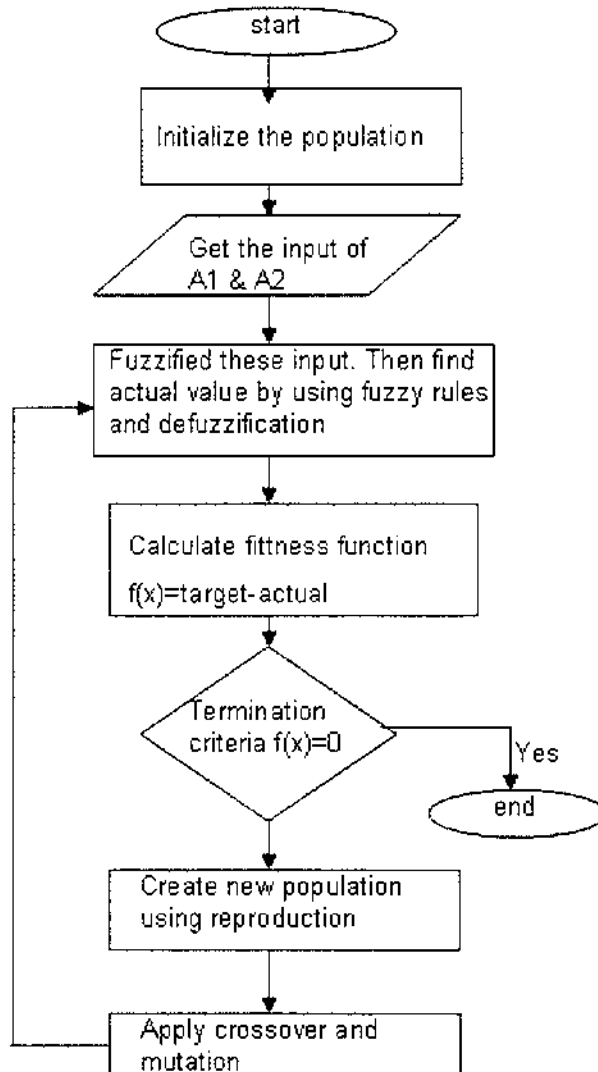
Figure 5.5 Flowchart

Number of substring

Population size   = 15

Number of gene in a chromosome   = 18(r 1 to r18)

Table 5.4 Fuzzy Optimization Using Genetic Algorithm

Al	VS	S	M	L	VL
Population	r1	r2	r3	r4	r5
1	1.25	0.84	3.64	0.4	1.55
2	0.15	0.74	3.63	0.4	2.5
3	**0.9**	**0.55**	**2.0**	**3.1**	**2.515**
4	0.315	1.46	3.63	0.6	2.5
5	0.15	1.56	0.75	3.6	2.5
6.	1.3	2.2	2.75	3.6	4.3
7	0.25	0.45	3.2	0.1	1.78
8	0.32	0.22	1.6	0.2	1.54
9	0.4	0.4	1.8	0.3	2
10	0.86	0.54	2.75	3.6	3.4
11	0.5	0.4	0.9	1.2	1.8
12	1.3	0.7	3.2	0.7	1.7
13	0.35	0.84	3.63	0.9	2.5
14	0.512	0.46	2.63	0.6	1.5
15	0.42	0.62	1.8	1.2	2.54

Table 3.5 Fuzzy Optimization Using Genetic Algorithm

A2	VS	S	M	L	VL
Population	r6	r7	r8	r9	r10
1	0.415	2.72	1.65	2.4	1.4
2	1.315	2.72	6.65	0.4	2.4
3	**0.415**	**0.27**	**3.145**	**2.72**	**1.65**
4	1.5	1.32	6.65	0.12	2.4
5	0.5	0.732	3.65	0.12	4.4
6	1.34	2.32	2.76	0.24	4.4
7	1.45	3.23	2.90	0.4	3.2
8	1.7	1.5	2.2	0.2	2
9	1.1	0.98	0.4	3.2	1.5
10	0.535	0.265	2.76	0.24	3.3
11	0.6	1.2	0.4	2.0	1.5
12	0.615	2.9	1.9	2.4	1.4
13	2.315	3.1	7.0	0.6	2.3
14	1.8	1.32	5.65	0.12	2.4
15	1.7	1.5	2.6	0.4	2.7

Output	0	1	2	3	4	5	6	7
Population	r11	r12	r13	r14	r15	r16	r17	r18
1	0.78	0.38	0.56	0.15	0.44	0.73	0.12	0.42
2	0.28	0.48	0.66	0.15	0.44	0.32	0.58	0.42
3	**0.1415**	**0.5265**	**0.68**	**0.565**	**0.705**	**0.605**	**0.45**	**0.625**
4	0.38	0.21	0.4	0.45	0.54	0.73	0.24	0.53
5	0.63	0.51	0.5	0.5	0.54	0.5	0.5	0.52
6	0.5	0.51	0.5	0.43	0.54	0.5	0.5	0.52
7	0.3	0.4	0.7	0.2	0.4	0.5	0.54	0.4
8	0.5	0.4	0.45	0.65	0.5	0.6	0.4	0.6
9	0.34	0.6	0.35	0.54	0.34	0.44	0.65	0.71
10	0.025	0.326	0.46	0.612	0.49	0.63	0.54	0.56
11	0.54	0.55	0.45	0.8	0.32	0.56	0.35	0.56
12	0.78	0.38	0.56	0.15	0.44	0.73	0.12	0.42
13	0.28	0.58	0.56	0.35	0.44	0.32	0.58	0.62
14	0.48	0.21	0.24	0.53	0.54	0.73	0.24	0.53
15	0.75	0.34	0.45	0.65	0.35	0.6	0.4	0.6

In this project first the semi-circular membership function center is assumed. Using genetic algorithm, the radius of the membership function is only optimized. The tables 5.4-5.6 give the various radius values; among these the best fit is selected by choosing the lowest error in the Tables. The A1 semicircular membership functions center are assumed as −56.32, -55.05, -52.6, -48.2 and −43.315. The A2 semicircular membership functions center are assumed as −62.085, -61.43, -58.145, -52.72, -49.35. Similarly the output semi-circular membership functions centers are assumed as 0,1,2,3,4,5,6 and 7.

Comparison of the fuzzy approach using conventional method and optimization technique using genetic algorithm for fault detection is shown in Table 5.7. From the table it is inferred that the error percentage compared with the conventional technique is reduced in optimization technique using genetic algorithm.

Table 5.7 Comparison of Conventional and Optimized method

Techniques	r1	r2	r3	r4	r5	r6	r7	r8	r9	r10	r11	r12	r13	r14	r15	r16	r17	r18	% Error
Conventional	0.86	0.54	2.75	3.6	3.4	0.535	0.265	2.76	0.24	3.3	0.025	0.326	0.455	0.612	0.49	0.63	0.54	0.56	1.8
Optimized	0.9	0.55	2	3.1	2.515	0.415	0.27	3.145	2.72	1.65	0.142	0.527	0.68	0.565	0.705	0.605	0.45	0.63	0.0

58

An On-Line broken rotor bar and end-ring fault detection scheme has been developed for three phase squirrel cage induction motor. The stator current spectrum of broken rotor bar and end-ring are recorded using real time analyzer and the harmonic amplitude levels at the particular frequency (Here 46Hz and 54Hz) are monitored using MATLAB. The amplitude levels were given as input to fuzzy logic. The output of the fuzzy logic will indicate the condition of the rotor like one broken rotor bar or zero broken bar.

6.1 SOFTWARE DESIGN

A similar software approach is done to find the status of both the end-ring and rotor bars by checking their amplitudes at the specified frequencies using MATLAB software package.

6.1.1 Algorithm

Step 1:   Start.

Step 2:   To record current signal from the sound card.

Step 3:   Perform FFT analysis.

Step 4:   Extract magnitude at the particular frequency.

Step 5:   Perform fuzzy diagnosis.

Step 6:   Display the status of End-ring and Rotor bar.
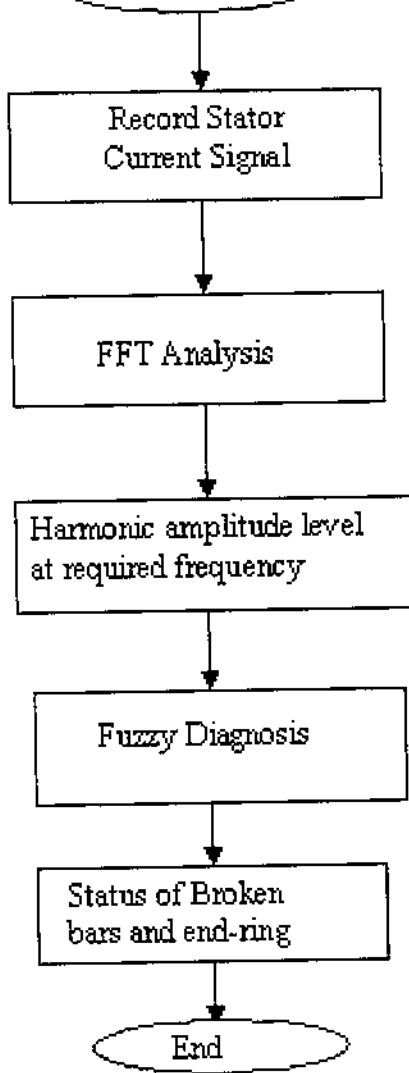
Figure 6.1 Flowchart of Software algorithms

6.2 PROGRAM

function varargout = flab(varargin)

    gui_Singleton = 1;

    gui_State = struct('gui_Name',   mfilename, ...

               'gui_Singleton', gui_Singleton, ...

               'gui_OpeningFcn', @flab_OpeningFcn, ...

               'gui_OutputFcn', @flab_OutputFcn, ...

               'gui_LayoutFcn', [] , ...

               'gui_Callback', []);

    if nargin && ischar(varargin{1})

```matlab
if nargout
    [varargout{1:nargout}] = gui_mainfcn(gui_State, varargin{:});
else
    gui_mainfcn(gui_State, varargin{:});
end
function flab_OpeningFcn(hObject, eventdata, handles, varargin)
    handles.output = hObject;
    guidata(hObject, handles);
    global FLAG;
    FLAG=1;
    set(handles.stopf,'Enable','off');
    function varargout = flab_OutputFcn(hObject, eventdata, handles)
    varargout{1} = handles.output;
function startf_Callback(hObject, eventdata, handles)
    set(handles.startf,'Enable','off');
    set(handles.stopf,'Enable','on');
    global FLAG;
    if(FLAG==0)
        FLAG=1;
    end
    pause(0.01);
    while FLAG==1
        eval('flab("xyz_Callback",gcbo,[],guidata(gcbo))');
        pause(0.01);
    end

function stopf_Callback(hObject, eventdata, handles)
    global FLAG;
    set(handles.startf,'Enable','on');
    set(handles.stopf,'Enable','off');
    FLAG=0;
```

```matlab
close

function forty_Callback(hObject, eventdata, handles)
function forty_CreateFcn(hObject, eventdata, handles)
    if ispc
        set(hObject,'BackgroundColor','white');
    else
        set(hObject,'BackgroundColor',get(0,'defaultUicontrolBackgroundColor'));
    end
function fifty_Callback(hObject, eventdata, handles)
function fifty_CreateFcn(hObject, eventdata, handles)
    if ispc
        set(hObject,'BackgroundColor','white');
    else
        set(hObject,'BackgroundColor',get(0,'defaultUicontrolBackgroundColor'));
    end
function eresult_Callback(hObject, eventdata, handles)
function eresult_CreateFcn(hObject, eventdata, handles)
    if ispc
        set(hObject,'BackgroundColor','white');
    else
        set(hObject,'BackgroundColor',get(0,'defaultUicontrolBackgroundColor'));
    end
function bresult_Callback(hObject, eventdata, handles)
function bresult_CreateFcn(hObject, eventdata, handles)
    if ispc
        set(hObject,'BackgroundColor','white');
    else
        set(hObject,'BackgroundColor',get(0,'defaultUicontrolBackgroundColor'));
    end


function xyz_Callback(hObject, eventdata, handles)
    Fs = 96000;
    y = wavrecord(3*Fs,Fs,'double');
```

```
size=131072*2;
Y = fft(y.size);
Pyy = abs(Y)/size;
Plog = 20 * log10(Pyy);
f = Fs*(1:size)/size;
% -- MAGNITUDE AT 46 Hz -- %
x = (f-46)/46;
for i=1:size
    if( x(i) <0)
        x(i)=x(i)*(-1);
    end
end
[c,l]=min(x);
abc = Plog(l);
% -- MAGNITUDE AT 54 Hz -- %
z = (f-54)/54;
for j=1:size
    if( z(j) <0)
        z(j)=z(j)*(-1);
    end
end
[d,m]=min(z);
def = Plog(m);
set(handles.forty,'String',abc);
set(handles.fifty,'String',def);
plot(f(10:400),Plog(10:400));
fismat1 = readfis('one.fis');
out1 = evalfis(abc,fismat1);
if (out1<0.1)
    out1='0 BAR BROKEN';
else
    if (out1>0.9)
```

```
        if(out1 < 0.6 && out1>0.4)
            out1='4 BROKEN BAR';
        end
    end
end
set(handles.bresult,'String',out1);
set(handles.eresult,'String','0');
```
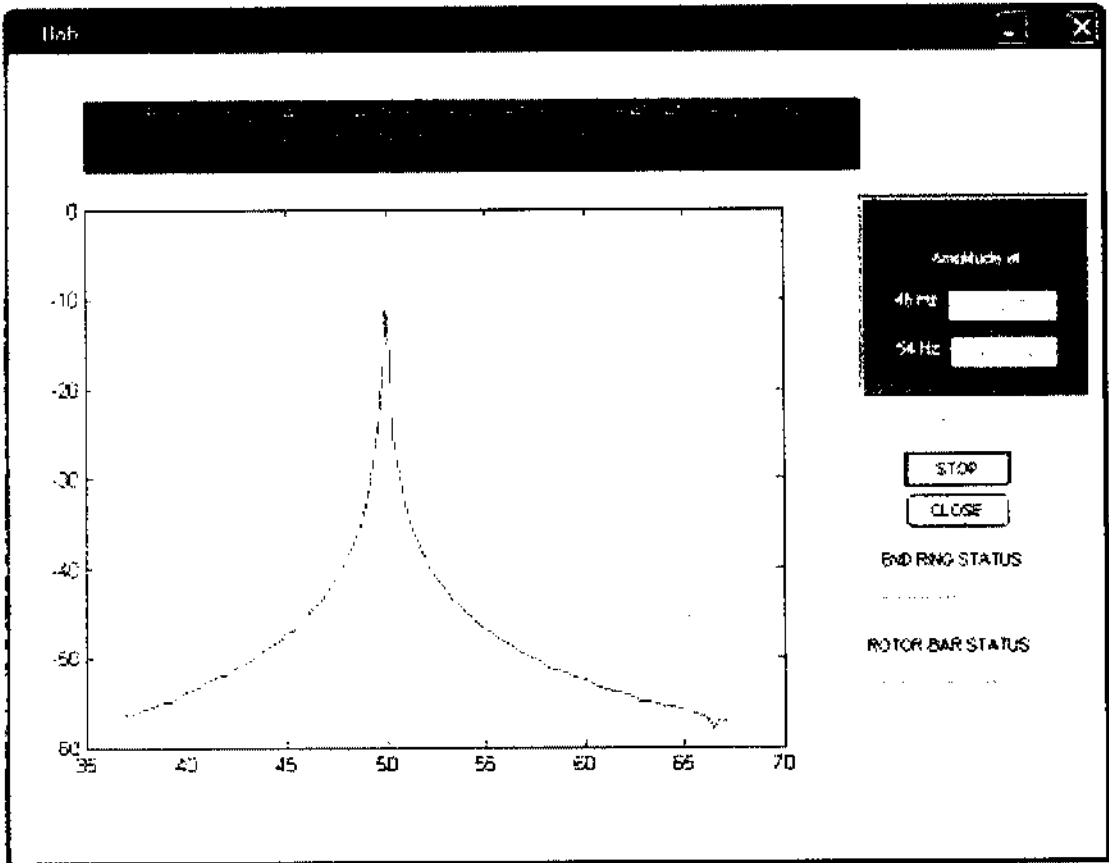
6.3 PICTURE OF THE SOFTWARE

Figure 6.2 Picture of the Software

7.1 CONCLUSION

The frequency components of the stator current have been experimentally analyzed for broken rotor bar and broken end-rings. Then, this work suggests that the non-invasive diagnostic system of motor current signature analysis monitoring can lead to an improvement in the reliability of diagnosis of rotor broken bars and connectors. This fault detection scheme can also be extended to other types of motors. Semi-circular membership function has been used and proved that it is better than other conventional membership functions for fuzzy fault diagnosis technique. Using genetic algorithm the fuzzy membership functions were optimized. The on-line fault detection scheme was done by fuzzy logic approach upto seven broken bars.

7.2 FUTURE SCOPE

The fault detection scheme can be carried out using neuro-fuzzy techniques. While neural networks can be used to correctly monitor the condition of a motor, they cannot provide general heuristic or qualitative information about what contributes to a fault. For these reasons, fuzzy logic can be used to provide a general heuristic solution to a particular problem with the use of general heuristic knowledge about the problem. However, a priori knowledge about the system is necessary to develop the fuzzy rules and membership functions. So this problem can be solved by integrating the use of fuzzy logic within the neural network structure.

Fuzzy rules can be optimized using genetic algorithm. And also this fault detection scheme can be extended to other types of motors.

[1] Peter Vas, "Artificial Intelligence-Based Electrical Machines and Drives", Clarendron press, Oxford, 1999.

[2] Mo-Yuen Chow, "Methodologies of using Neural Network and Fuzzy Logic technologies for Motor Incipient Fault Detection",World Scientific Publishing Co. Pte.Ltd. Singapore, 1997.

[3] Laurene Fausett, "Fundamentals of Neural Networks", Pearson Education Pte. Ltd., Delhi.2004.

[4] G.B.Kliman et al., "Non-invasive Detection of Broken Rotor Bars in Operating Induction Motors." IEEE Trans. Energy conv., vol. 3, No.4,pp.873-879,Dec. 1988.

[5] H.A. Toliyat and T.A.Lipo, "Transient Analysis of Cage Induction Machines under Stator, Rotor Bar and End-ring Faults", IEEE Trans. Energy conv., vol. 10, no.2.,pp.241-247, June 1995.

[6] A.Keyhani and S.M. Miri,"Observers for Tracking of Synchronous Machine Parameters and Detection of Incipient Faults", IEEE Trans. Energy conv., vol. 1, no.2, 1986.

[7] G.C.Stone and J.F.Lyles, "A Thermal Cycling Type Test for Generator Stator Winding Insulation", IEEE Trans. Energy conv., vol. 6, no.4, pp 707-712,1991.

[8] M.E.H.Benbouzid et al.,"Large Induction Machines Faults Monitoring by Power Line Signal Spectral Analysis", Proceedings of the International Conference on Acoustical and Vibratory Surveillance Methods and Techniques", Senlis (France), 1998.

[9] W.T.Thomson, "On-line Current Monitoring To Detect Electrical and Mechanical Faults in Three-phase Induction Motors", Proceedings of the IEE International Conference on Life Management of Power Plant, London (UK), pp66-74, 1994.

[10] M.Y.Chow, "The Advantages of Machine Fault Detection Using Artifitial Neural Network and Fuzzy Logic Technologies", Proceedings of the IEEE International Conference on Industrial Technology,Guangzhou(china),pp 83-87,1994.

[11]Humberto Henao, Hubert Razik and Gerard-Andre Capolino, "Analytical Approach of the Stator Current Frequency Harmonics Computation for Detection of Induction Machine Rotor Faults", IEEE Trans. Industry App., vol. 41, no.3, pp.801-807, June 2005.

Coupled Finite Element State space Modeling Approach", IEEE Trans. Energy conv., vol. 14, No.4.,pp.1167-1176, Dec. 1999.

[13] Bulent Ayhan, Mo-Yuen Chow and Myung-Hyun Song, "Multiple Signature Processing Based Fault Detection Schemes for Broken Rotor Bar in Induction Motors", IEEE Trans. Energy conv., vol.20, no.2, pp.336-347, June 2005.

[14] Fiorenzo Filippetti, Giovanni Franceschini, and Peter Vas, "Recent Development of Induction Motor Drives Fault Diagnosis Using AI Techniques", IEEE Trans. Industrial Electronics., vol. 47, No.5.,pp.994-1003, Oct. 2000.

[15] ST.J.Manolas and J.A.Tegopoulos, "Analysis of Squirrel Cage Induction Motor With Broken Bars and Rings", IEEE Trans., Energy conv., vol.14, no.4, pp.1300-1305, Dec 1999.

[16] J.F.Bangura, N.A.Demerdash, "Comparison Between Characterization and Diagnosis of Broken Bars/End-Ring Connectors and Airgap Eccentricities of Induction Motors in ASD's Using a Coupled Finite Element-State Space Method", IEEE Trans. on Energy conv., vol. 15, no.1, pp.48-56, Mar 2000.

[17] Behrooz Mirafzal et al., "Induction Machine Broken-Bar Fault Diagnosis Using the Rotor Magnetic Field Space-Vector Orientation", IEEE Trans. Industry App., vol. 40, no.2, pp.534-542, March 2004.

[18] Behrooz Mirafzal et al., "Effects of Load Magnitude on Diagnosing Broken Bar Faults in Induction Motors Using the Pendulous Oscillation of the Rotor Magnetic Field Orientation ", IEEE Trans. Industry App., vol. 41, no.3, pp.771-783, May 2005.

[19] R.Rajesh et al., "Semi-Circular Membership Function for Fuzzy Systems", Journal of the CSI., Vol.33,no.1, pp 40-47,March 2003

[20] Jafar Milimonfared, Honayoun Meshgin Kelk and Subhasis Nandi, 'A Novel Approach for Broken- Rotor – Bar Detection in Cage Induction Motor', IEEE Transaction-Industry Application, Vol 35, No. 5, Pp 1000 – 1005,1999.